

Shape Alignment via Allen-Cahn Nonlinear-Convection

Daniel Solano^{1,2,3}, Jerome Darbon², and Laurent Younes^{1,3}

¹Johns Hopkins University, Department of Applied Mathematics and Statistics, Baltimore, USA

²Brown University, Division of Applied Mathematics, Providence, USA

³Johns Hopkins University, Center for Imaging Science, Baltimore, USA

April 24, 2025

Abstract

This paper demonstrates the impact of a phase field method on shape registration to align shapes of possibly different topology. It yields new insights into the building of discrepancy measures between shapes regardless of topology, which would have applications in fields of image data analysis such as computational anatomy. A soft end-point optimal control problem is introduced whose minimum measures the minimal control norm required to align an initial shape to a final shape, up to a small error term. The initial data is spatially integrable, the paths in control spaces are integrable and the evolution equation is a generalized convective Allen-Cahn. Binary images are used to represent shapes for the initial data. Inspired by level-set methods and large diffeomorphic deformation metric mapping, the controls spaces are integrable scalar functions to serve as a normal velocity and smooth reproducing kernel Hilbert spaces to serve as velocity vector fields. The existence of mild solutions to the evolution equation is proved, the minimums of the time discretized optimal control problem are characterized, and numerical simulations of minimums to the fully discretized optimal control problem are displayed. The numerical implementation enforces the maximum-bounded principle, although it is not proved for these mild solutions. This research offers a novel discrepancy measure that provides valuable ways to analyze diverse image data sets. Future work involves proving the existence of minimums, existence and uniqueness of strong solutions and the maximum bounded principle.

Keywords: Phase-field Model; Large Diffeomorphic Deformation Metric Mapping; Level Set Methods, Allen-Cahn Equation; Optimal Control; Bounded Maximum Principle

1 Introduction

In his seminal treatise “On Growth and Forms” [53], D’Arcy Thompson introduced the fundamental principle of analyzing the similarities between two shapes through the construction of transformations mapping one of them into the other. This principle was later formalized in Grenander’s pattern theory [30, 29], the theory developing into practical tools with the introduction of diffeomorphic registration [66] and, among others, the large deformation diffeomorphic mapping algorithm [36, 11, 54, 55, 20, 7], or LDDMM. This approach, along with many others targeting diffeomorphic registration [6, 24, 17, 59, 5], has been used for applications that extract information from shape changes, including, in particular, medical studies based on computational anatomy [31].

These methods respect the basic paradigm of D’Arcy Thompson theory of transformations in that they evaluate, for comparison purposes, the “simplest” diffeomorphic transformation mapping one shape onto another. Restricting to such transformations has several advantages, one of the foremost being the structure of the diffeomorphism groups and the existence of well-studied Riemannian metrics [4, 40], with transformations

conveniently represented as flows of ordinary differential equations [16, 55, 66]. In addition, diffeomorphisms are easily interpretable, as they can register target shapes to a fixed “template” allowing for the transport of existing information (such as region labeling) from the latter to the former. Moreover, morphometric measures based on the deformation Jacobian are easily computable and can be used in further analysis [5].

Shape spaces represented as sets of diffeomorphic transformations of a template can be build to include a wild variety of objects, albeit all within the same topological class. Eliminating this topological constraint is challenging, however, as it may require to relinquish many of the properties that were just listed. Non-diffeomorphic comparison between images have been introduced in the context of metamorphosis [41, 57, 33, 47, 46], which estimates transformations between images by optimizing displacements both in space and image intensity. There is no canonical modification of this approach to comparing shapes, defined as curves or surfaces, however, in that running metamorphosis between two images with given zero level, would depend on the choice made for this representation, and not on the level sets themselves. This limitation is partially addressed in [34], in which shapes are embedded in a much larger space of varifolds, which can be described, in codimension one, as products of measures on \mathbb{R}^d (the varifold weight) and transition probabilities from \mathbb{R}^d to the unit sphere. The metamorphosis mechanism is then applied to the weight component of the varifold. Since not all varifolds correspond to geometric curves or surfaces, this representation does not define, however, shape trajectories. Other work addressing the partial matching problem also include [3, 51].

Of course, the ability to numerically generate topological changes by tracking the level sets of a function satisfying partial differential equations has a long history [44, 43, 45, 48], but such processes, which have found a wide range of applications in shape regularization, using, in particular, mean-curvature motion [25, 28, 22], and in shape segmentation [14, 60, 15, 39], have had limited impact in shape analysis, mainly because these equations simplify their solutions (and the associated level sets) in a non-reversible way, which limits their usefulness in transporting spatial information.

In this paper, we provide a new strategy for shape analysis, in which a template shape is controlled by a combination of a diffeomorphic and normal flows while being submitted to a small amount of mean-curvature motion, in order to align with a target shape that is only subject to the mean-curvature motion. Shapes being described as two- or three-dimensional sets with finite Lebesgue measure, their evolution is described using a nonlinear parabolic partial differential evolution equation of their characteristic functions. We prove the global existence and uniqueness of this parabolic equation—specifically a generalized convective Allen Cahn equation. We set up a time discretization of an optimal control problem with running and terminal cost and prove a Pontryagin’s maximum principle for this problem. And finally, we show some numerical results in which we transform the characteristic function of an initial shape into the mollified characteristic function of a target shape with possibly different topology. Our critical contribution is in designing a meaningful discrepancy measure between shapes that is based on the minimal energy spent transforming one shape into another shape, regardless of whether they share the same topology.

Section 2.3 provides the statement of our main theorem, preceded by the necessary definitions and background results, while Section 3 sets up the optimal control problem implemented in our experiments. The main theorem is proved in Section 4. Section 5 describes the discrete-time implementation of the method as an optimal control problems and make explicit the discrete Pontryagin maximum principle providing necessary conditions satisfied by solutions. Finally, Section 6 provides experimental illustrations of the method.

2 Main theorem

2.1 Summary of notation

If B is a Banach space and $r \geq 1$, $L^r(\Omega, B)$ is the space of r -integrable functions (in the Bochner sense) from a measured space Ω to B with the usual L^r norm that we will denote $\|\cdot\|_{L^r}$. The notation is reduced to $L^r(\Omega)$ when $\Omega = \mathbb{R}$. We will also only write L^r when Ω and B are clear from the context. Given $\ell \geq 1$, we let $\ell^* = \ell/(\ell - 1)$ such that $1/\ell + 1/\ell^* = 1$.

The spaces $W^{k,r}(\mathbb{R}^d, \mathbb{R}^q)$ are the usual Sobolev spaces of functions $h : \mathbb{R}^d \rightarrow \mathbb{R}^q$ with all partial derivatives

in L^r , and norm

$$\|h\|_{W^{k,r}} = \left(\sum_{\alpha, |\alpha| \leq k} \|\partial_\alpha h\|_r^r \right)^{1/r}$$

where the sum is over all multi-indexes of order k or less, and ∂_α refers to partial derivatives with respect to coordinates indexed by the indexes in α . We will only write $W^{k,r}$ when d and q are clear from context, and we note that $W^{0,r} = L^r$.

The Banach space of bounded k -times continuously differentiable functions from \mathbb{R}^d to \mathbb{R}^q is denoted $C^k(\mathbb{R}^d, \mathbb{R}^q)$, with norm

$$\|h\|_{C^k} = \max_{\alpha: |\alpha| \leq k} \sup_{x \in \mathbb{R}^d} |h(x)|$$

(where $|y|$ denotes the Euclidean norm in finite dimensional spaces). The space $C_0^k(\mathbb{R}^d, \mathbb{R}^q)$ of functions that tend to 0 at infinity is the completion in $C^k(\mathbb{R}^d, \mathbb{R}^q)$ of compactly supported functions. Again, we will only write C^k and C_0^k when domains and codomains are clear from context.

We let V be a Hilbert space of vector fields that is continuously embedded in $C^1(\mathbb{R}^d, \mathbb{R}^d)$. Within large diffeomorphic deformation metric mapping, LDDMM, metrics (distances) are built between embeddings $S_0, S_1 \subset \mathbb{R}^d$ of a chosen C^1 oriented manifold M . For these $S_0, S_1 \subset \mathbb{R}^d$, one determines a $v \in L^2([0, 1], V)$ with minimal norm such that its flow, which satisfies¹

$$\varphi_{0t}^v(x) = x + \int_0^t v(s, \varphi_{0s}^v(x)) ds,$$

maps S_0 to S_1 at time one, i.e., $\varphi_{01}^v(S_0) = S_1$. The minimum norm, written $d_V(S_0, S_1) \in [0, +\infty]$, is a metric on the space of embeddings of M , written $\text{Emb}(M, \mathbb{R}^d)$; see [13, 65, 11, 26, 36, 58] for more details on LDDMM and [9, 10] for an overview of shape analysis methods. In practice, one relaxes the boundary conditions into a soft end-point problem: minimize

$$\int_0^1 \|v(t)\|_V^2 dt + U(\varphi_{01}^v), \quad v \in L^2([0, 1], V),$$

where $U : C^1(\mathbb{R}^d, \mathbb{R}^d) \rightarrow \mathbb{R}$ is a continuous function bounded from below, which penalizes the lack of alignment between S_1 and $\varphi_{01}^v(S_0) = S_1$. Various choices are possible; check Chapters 10 and 11 of [66] for more details.

2.2 Useful properties of convolutions

The convolution between two functions f and g is denoted $f \star g$. It is a bilinear mapping from $L^1 \times L^r$ to L^r , which is bounded with [12]

$$\|f \star g\|_{L^r} \leq \|f\|_{L^1} \|g\|_{L^r}. \quad (1)$$

We denote by η_τ the Gaussian function $x \mapsto \frac{\exp(-|x|^2/2\tau^2)}{(2\pi)^{d/2}\tau^d}$. The convolution by η_τ is a bounded linear mapping between various pairs of states, as stated in the following lemma.

Lemma 1. (Chapter 15, 1.15, Third Equation, [52]) *Let $q \geq \tilde{q} \in [1, \infty)$, $k \geq l \in \mathbb{R}$, and $\tau > 0$. Then $f \mapsto \eta_\tau \star f$ is a bounded linear mapping from $W^{l, \tilde{q}}(\mathbb{R}^d)$ to $W^{k, q}(\mathbb{R}^d)$ with, for some $C > 0$,*

$$\|\eta_\tau \star f\|_{W^{k, q}} \leq C\tau^{-2\gamma} \|f\|_{W^{l, \tilde{q}}},$$

$f \in W^{l, \tilde{q}}(\mathbb{R}^d)$ and where

$$\gamma = \frac{d}{2} \left(\frac{1}{\tilde{q}} - \frac{1}{q} \right) + \frac{1}{2}(k - l).$$

¹We will denote time-dependent vector fields either as $t \mapsto v(t)$ where $v(t)$ is a vector field or $t \mapsto v(t, \cdot)$, which is unambiguous within the spaces we will consider.

Proof. We give a rapid proof of this result for completeness. Let a be a d -dimensional multi-index with $|a| \leq k$ and choose b with $b \leq a$ and $|b| = \min(|a|, l)$. Let $c = a - b$, so that $|c| \leq k - l$. We have $\partial_a(\eta_\tau \star f) = (\partial_c \eta_\tau) \star (\partial_b f)$, and we let below $\bar{\eta}_\tau = \partial_c \eta_\tau$ and $g = \partial_b f$. We have $\bar{\eta}_\tau \star g = (\bar{\eta}_\tau^{1/\bar{q}^*} \bar{\eta}_\tau^{1/\bar{q}}) \star g$ yielding

$$|\bar{\eta}_\tau \star g| \leq \|\bar{\eta}_\tau\|_{L^1}^{1/\bar{q}^*} |\bar{\eta}_\tau \star g^{1/\bar{q}}|^{1/\bar{q}}.$$

This shows that

$$\|\bar{\eta}_\tau \star g\|_{L^q} \leq \|\bar{\eta}_\tau\|_{L^1}^{1/\bar{q}^*} \|\bar{\eta}_\tau \star g^{1/\bar{q}}\|_{L^{q/\bar{q}}} \leq \|\bar{\eta}_\tau\|_{L^1}^{1/\bar{q}^*} \|g^{1/\bar{q}}\|_{L^1} \|\bar{\eta}_\tau\|_{L^{q/\bar{q}}}^{1/\bar{q}} = \|\bar{\eta}_\tau\|_{L^1}^{1/\bar{q}^*} \|\bar{\eta}_\tau\|_{L^{q/\bar{q}}}^{1/\bar{q}} \|g\|_{L^q}$$

To conclude the proof, one uses the fact that $\eta_\tau(x) = \tau^{-d} \eta_1(x/\tau)$, which implies that $\bar{\eta}_\tau(x) = \tau^{-d-|c|} \bar{\eta}_1(x/\tau)$ and $\|\bar{\eta}_\tau\|_{L^r} = \tau^{-d-|c|+d/r} \|\bar{\eta}_1\|_{L^r}$ for $r \geq 1$. \square

We will also need similar properties with C_0^k instead of $W^{k,q}$.

Lemma 2. *Let $\tilde{q} \in [1, \infty)$, $k \geq l \in \mathbb{R}$, and $\tau > 0$. Then $f \mapsto \eta_\tau \star f$ is a bounded linear mapping from $W^{l,\tilde{q}}(\mathbb{R}^d)$ to $C_0^k(\mathbb{R}^d)$ with, for some $C > 0$,*

$$\|\eta_\tau \star f\|_{C^k} \leq C \tau^{-2\gamma} \|f\|_{W^{l,\tilde{q}}},$$

$f \in W^{l,\tilde{q}}(\mathbb{R}^d)$ and where

$$\gamma = \frac{d}{2\tilde{q}} + \frac{1}{2}(k-l).$$

It is also a bounded linear mapping from $C_0^l(\mathbb{R}^d)$ to $C_0^k(\mathbb{R}^d)$ with, for some $C > 0$,

$$\|\eta_\tau \star f\|_{C^k} \leq C \tau^{-2\gamma} \|f\|_{C^l},$$

$f \in C^l(\mathbb{R}^d)$ and where

$$\gamma = \frac{1}{2}(k-l).$$

Proof. The proof is similar to that above, essentially taking $q = \infty$, and $\tilde{q} = \infty$. \square

2.3 Main result

Definition 1. *Define the C^1 function $I : \mathbb{R} \rightarrow \mathbb{R}$, for some $W > 0$, by*

$$I(\xi) = W \xi^2 (\xi - 1)^2 (\xi - 1/2) \cdot \mathbf{1}_{[0,1]}(\xi) \quad (2)$$

Let $p \in (2, \infty]$, $r \in (\frac{dp}{p-2}, \infty]$, and $\sigma > 0$ be fixed real numbers. All constants considered below may depend of these numbers and on W .

Let $\mathcal{U} = L^p([0, 1], L^r(\mathbb{R}^d))$, and $\mathcal{V} = L^p([0, 1], V)$.

Our main evolution equation is the following generalized convective Allen-Cahn equation. It is a semi-linear parabolic PDE whose mild solutions can be written in integral form by using the heat kernel $\eta_{\sigma\sqrt{t}}$ as a contraction semigroup generator; see [52], Chapter 15.1, [21] 7.4, [64] Chapter 4, [32]).

Theorem 1. *Suppose $f_0 \in L^{r^*}(\mathbb{R}^d)$, $u \in \mathcal{U} = L^p([0, 1], L^r(\mathbb{R}^d))$, and $v \in \mathcal{V} = L^p([0, 1], V)$. There is a unique mild solution $f \in C^0([0, 1], L^{r^*}(\mathbb{R}^d)) \cap C^0((0, 1], W^{1,r^*}(\mathbb{R}^d))$ to the differential equation*

$$\partial_t f(t, x) = \frac{\sigma^2}{2} \Delta f(t, x) + I(f(t, x)) + u(t, x) |\nabla f(t, x)| - v(t, x)^T \nabla f(t, x), \quad (t, x) \in [0, 1] \times \mathbb{R}^d \quad (3)$$

given by the integral equation

$$f(t) = \eta_{\sigma\sqrt{t}} \star f_0 + \int_0^t \eta_{\sigma\sqrt{t-s}} \star (I(f(s)) + u(s)|\nabla f(s)| - v^T(s)\nabla f(s)) ds,$$

which satisfies

$$\|f\|_P = \max \left(\sup_{t \in [0,1]} \|f(t)\|_{L^{r^*}}, \sup_{t \in (0,1]} \sqrt{t} \|f(t)\|_{W^{1,r^*}} \right) < \infty.$$

Moreover, $\lim_{t \rightarrow 0} f(t) = f_0$ in $L^{r^*}(\mathbb{R}^d)$.

Equation (3) provides our control system, with state f and control $(u, v) \in \mathcal{U} \times \mathcal{V}$. The following highlights the specific contributions of its terms.

1. We first note that, in the absence of control (when u and v are identically zero) and when f_0 is a characteristic function of some finite-measure $V \subset \mathbb{R}^d$, the function f evolves according to an Allen-Cahn equation,

$$\partial_t f = \frac{\sigma^2}{2} \Delta f + I(f), \quad f_0 = \mathbf{1}_V.$$

This equation approximates a mean curvature flow in the context of phase-field dynamics [18] as $W \rightarrow \infty$ in Eq. (2). The typical Allen-Cahn equation uses the negative of the derivative of the double well polynomial $\phi(\xi) = W\xi^2(\xi - 1)^2$ (for some $W > 0$) in order to push the phase-field toward the values 0 or 1. Here $I(\xi)$ has the same sign as $-\phi'(\xi)$ for $\xi \in [0, 1]$ and is C^1 and compactly supported, which provides numerical stability and an easier proof of Theorem 1.

2. This approximate mean-curvature flow regularizes our “ideal” control equation

$$\partial_t f + \nabla f^T v = |\nabla f| u \tag{4}$$

in which the l.h.s. is equal to $\partial_t(f \circ \varphi_{0t}^v) \circ (\varphi_{0t}^v)^{-1}$ where φ_{0t}^v is the flow associated with v , and the r.h.s. defines a normal flow of the level sets of f , with velocity u , which makes possible topological changes. For this reason, we will refer to v as the diffeomorphic control and u as the topological control. Equation (4) is reminiscent of the metamorphosis equation, as introduced in [41, 57, 56], that takes the form

$$\partial_t f + \nabla f^T v = u$$

with $u \in L^2([0, 1], L^2)$. This equation was introduced for image alignment and, unlike Eq. (4), the contribution of u does not have a clear geometric interpretation. While the existence of solutions for the metamorphosis system is easily deduced from $\partial_t(f \circ \varphi) = u \circ \varphi$, the analysis of Eq. (4) for general $u \in \mathcal{U}$ is, up to our knowledge, open, without the introduction of a regularizing term.

3. If we only set u to be identically zero and f_0 to be a characteristic function, then Eq. (3) is a a convective Allen-Cahn equation

$$\partial_t f = \frac{\sigma^2}{2} \Delta f + I(f) - \nabla f^T v, \quad f_0 = \mathbf{1}_V$$

which has recently been applied in elastic and viscoelastic surfaces in fluids [37]. Non-convergence results for this equation have been obtained if one couples it with a Navier-Stokes method [1], and it has been compared to convection via level-set methods where one resets an evolving distance function [27].

4. Suppose one sets $W = 0$, effectively setting $I = 0$, and $f_0 = d_{V^c}$ (the complement distance function of some bounded $V \subset \mathbb{R}^d$). Then Eq. (3) becomes

$$\partial_t f = \frac{\sigma^2}{2} \Delta f + |\nabla f| u - \nabla f^T v.$$

In this setting if the controls u, v were continuous in (t, x) and bounded, then this equation would be a vanishing viscosity method [23]. Moreover, if u were continuous and bounded and we sent $\sigma \rightarrow 0$ and if our initial data was Lipschitz continuous then we would be in the realm of viscosity solutions to Hamilton-Jacobi-Bellman PDEs [8, 42]. This method found its inception in [44] and the most widely used implementation is the ENO/WENO numerical scheme [50, 35].

For the proof of existence and uniqueness of mild solutions, we loosely follow the work [61, 62, 63], and the outline in [52], Chapter 15. Our problem differs from those studied there through the introduction of two integrable time-dependent terms, one of which is nonlinear; this results in a Lipschitz constant that is not uniform in t in our contraction mapping proof, requiring finer estimates. In addition, our case of $u \in L^p([0, 1], L^r(\mathbb{R}^d))$ is a weaker assumption than in the work [2, 38] of quasilinear parabolic PDEs.

3 Optimal control problem

Our objective function is defined as follows. Let $f_0, f_{\text{target}} \in L^{r^*}$ and suppose we have a C^1 functional $U : W^{1,r^*} \rightarrow [0, \infty)$ that is bounded below such that $U(f_{\text{target}}) = 0$. We fix a positive parameter C_{top} and minimize

$$E(u, v) = C_{\text{top}} \int_0^1 \|u(t)\|_{L^r}^p + \|v(t)\|_{\mathcal{V}}^p dt + U(f(1)) \text{ over } (u, v) \in \mathcal{U} \times \mathcal{V}$$

$$\text{subject to } f(1) = \eta_\sigma \star f_0 + \int_0^1 \eta_{\sigma\sqrt{1-s}} \star (I(f(s)) + u(s)|\nabla f(s)| - v(s)^T \nabla f(s)) ds$$

If such a minimum exists, denote it as $\rho_\sigma(f_0, f_{\text{target}})$. If the minimum exists when we reverse the roles of f_{target} and f_0 , we define the σ -discrepancy measure by

$$d_\sigma(f_0, f_{\text{target}}) = \min(\rho_\sigma(f_0, f_{\text{target}}), \rho_\sigma(f_{\text{target}}, f_0)).$$

By definition, $d_\sigma(f_0, f_{\text{target}})$ is symmetric and for choice U it also has the property that $f_0 = f_{\text{target}} \implies d_\sigma(f_0, f_{\text{target}}) = 0$. However, we do not claim it satisfies the triangle inequality.

As we show in the coming section, we require $\sigma > 0$ to have existence and uniqueness of mild solutions so that the problem may be well posed. We display numerical simulations in the last section of this paper.

In our experiments, we will compare the numerical minimums of E as we send C_{top} to infinity. We do this in order to qualitatively study how much of the alignment of f_0 and f_{target} can be contributed to the large diffeomorphic deformation geometric change caused by v and the non-smooth, geometric and topological change caused by u . We consider the parabolic orbits in W^{1,r^*} of the smoothed characteristic function that are smoothly convected by v , non-smoothly convected by u , and smoothed out by the semi-group generator η_σ . This is in contrast to LDDMM, where one only seeks a minimal $v \in \mathcal{V}$ to align the initial volume $V_0 \subset \mathbb{R}^d$ to a target volume $V_{\text{target}} \subset \mathbb{R}^d$ via the orbit $1_V \mapsto 1_{(\varphi_{01}^v)^{-1}(V)}$.

Due to I and η_σ , the initial data is also undergoing an approximate mean curvature flow ([18]), so the shape also changes slightly “for free.” So, all things considered, we are combining LDDMM, level set methods, and phase-field dynamics by using this generalized convective Allen-Cahn evolution equation for shape alignment via a soft-end point optimal control problem.

4 Existence and Uniqueness of Mild Solutions

We prove Theorem 1 in the following way.

1. Prove the existence of a “short-time” solution for small enough $T \in (0, 1]$ (Theorem 2 below).
2. Show that a uniform partition of $[0, 1]$ exists with partition mesh $\Delta t < T$ that satisfies a condition that depends on the norms of u, v .

3. Stitching several “short-time” fixed point solutions of a single u, v to create the global solution.

We will use Lemma 1 in the following special cases that we state as a corollary for easier reference.

Corollary 1. *We let $\epsilon \in \{0, 1\}$.*

(i) *There exists $C_0 > 0$ (that depends on d and σ) such that, for all $f \in L^{r^*}$,*

$$\|\eta_{\sigma\sqrt{t}} \star f\|_{W^{\epsilon, r^*}} \leq C_0 t^{-\epsilon/2} \|f\|_{L^{r^*}} \quad (5a)$$

(ii) *There exists $C_1 > 0$ (that depends on d and σ) such that, for all $f \in L^1$,*

$$\|\eta_{\sigma\sqrt{t}} \star f\|_{W^{\epsilon, r^*}} \leq C_1 t^{-\epsilon/2 - \gamma_1} \|f\|_{L^1} \quad (5b)$$

with $\gamma_1 = dr/2$.

We will use the following notation and remarks.

1. Let C_I denote the Lipschitz constant of I (one can take $C_I = W/16$). Let C_V be a constant for which

$$\|w\|_{C^1} \leq C_V \|w\|_V, \quad \forall w \in V.$$

2. One has, for $0 < a, b < 1$,

$$\int_0^t (t-s)^{-a} s^{-b} ds = \frac{\Gamma(1-a)\Gamma(1-b)}{\Gamma(2-(a+b))} t^{1-(a+b)} < \infty$$

where Γ is the classical Gamma function. The integral is unbounded as $a \rightarrow 1$ or $b \rightarrow 1$. Also remark that $\int_0^t (t-s)^{-\gamma} ds = t^{1-\gamma}/(1-\gamma)$ for $\gamma < 1$.

3. Let $\phi : [0, 1] \times (0, 1) \rightarrow \mathbb{R}$ be defined as

$$\begin{aligned} \phi(t, \gamma) &= \left(\int_0^t (t-s)^{-\gamma p^*} s^{-\frac{p^*}{2}} ds \right)^{1/p^*} \\ &= \left(\frac{\Gamma(1-\gamma p^*)\Gamma(1-p^*/2)}{\Gamma(2-(\gamma+1/2)p^*)} \right)^{1/p^*} t^{1/p^* - \gamma - 1/2}. \end{aligned}$$

Remark that there is a $K > 0$ such that

$$\max_{t \in [0, 1]} \left(\phi(t, 1/2), \sqrt{t}\phi(t, \gamma_1), \sqrt{t}\phi(t, \gamma_1 + 1/2) \right) < K, \quad C_V \left(\frac{1}{1-p^*/2} \right)^{1/p^*} < K.$$

Essential for this condition to be true is that $\frac{1}{p^*} - \frac{d}{2r} - \frac{1}{2} > 0$ which is true when $r > \frac{dp}{p-2}$ and $p > 2$, as assumed in Theorem 1.

4. For $T \in (0, 1]$, define P_T as the vector space of functions $f \in C^0([0, T], L^{r^*}(\mathbb{R}^d)) \cap C^0((0, T], W^{1, r^*}(\mathbb{R}^d))$ such that

$$\|f\|_{P_T} := \max \left(\sup_{t \in [0, T]} \|f(t)\|_{L^{r^*}}, \sup_{t \in (0, T]} \sqrt{t} \|f(t)\|_{W^{1, r^*}} \right) < \infty.$$

We note that $(P_T, \|\cdot\|_{P_T})$ is a Banach space and will use the notation

$$d(f, g)_{P_T} = \|f - g\|_{P_T}.$$

We will prove local existence of solutions as stated in the following theorem.

Theorem 2. Suppose $f_0 \in L^{r^*}(\mathbb{R}^d)$, $u \in \mathcal{U}$, and $v \in \mathcal{V}$. For small enough $T \in (0, 1]$, there is a unique solution $f \in C^0([0, T], L^{r^*}(\mathbb{R}^d)) \cap C^0((0, T], W^{1, r^*}(\mathbb{R}^d))$ to the integral equation

$$f(t) = \eta_{\sigma\sqrt{t}} \star f_0 + \int_0^t \eta_{\sigma\sqrt{t-s}} \star (I(f(s)) + u(s)|\nabla f(s)| - v(s)^T \nabla f(s)) ds, \quad \forall t \in [0, T] \quad (6)$$

which satisfies

$$\max \left(\sup_{t \in [0, T]} \|f(t)\|_{L^{r^*}}, \sup_{t \in (0, T]} \sqrt{t} \|f(t)\|_{W^{1, r^*}} \right) < \infty.$$

Moreover, $\lim_{t \rightarrow 0} f(t) = f_0$ in $L^{r^*}(\mathbb{R}^d)$

Proof. Recall that $p \in (2, \infty]$, $r \in (dp/(p-2), \infty]$, and $\sigma > 0$. Take $u \in \mathcal{U}$, $f_0 \in L^{r^*}$, and $v \in \mathcal{V}$. We set up a contraction mapping argument where the mild solution we seek is the unique fixed point of said mapping.

We fix $T \in (0, 1]$ and define $\Psi : P_T \rightarrow P_T$ by

$$\Psi(f)(t) = \eta_{\sigma\sqrt{t}} \star f_0 + \int_0^t \eta_{\sigma\sqrt{t-s}} \star (I(f(s)) + u(s)|\nabla f(s)| - v^T(s)\nabla f(s)) ds.$$

We also introduce the notation, for $u \in \mathcal{U}$, $v \in \mathcal{V}$:

$$\Psi_0 : t \mapsto \eta_{\sigma\sqrt{t}} \star f_0 \quad (7a)$$

$$\Psi_I(f) : t \mapsto \int_0^t \eta_{\sigma\sqrt{t-s}} \star I(f(s)) ds \quad (7b)$$

$$\Psi_u(f) : t \mapsto \int_0^t \eta_{\sigma\sqrt{t-s}} \star (u(s)|\nabla f(s)|) ds \quad (7c)$$

$$\Psi_v(f) : t \mapsto \int_0^t \eta_{\sigma\sqrt{t-s}} \star (v(s)^T \nabla f(s)) ds, \quad (7d)$$

so that $\Psi(f) = \Psi_0 + \Psi_I(f) + \Psi_u(f) - \Psi_v(f)$.

Preliminary lemma

We first prove the following lemma and its corollary.

Lemma 3. Let $\epsilon \in \{0, 1\}$. For $f, g \in C^0([0, T], L^{r^*}) \cap C^0((0, T], W^{1, r^*})$, one has, for all $t \in (0, T]$,

$$\int_0^t \|\eta_{\sigma\sqrt{t-s}} \star (I(f(s)) - I(g(s)))\|_{W^{\epsilon, r^*}} ds \leq C_0 C_I \int_0^t (t-s)^{-\epsilon/2} \|f(s) - g(s)\|_{L^{r^*}} ds \quad (8a)$$

$$\int_0^t \|\eta_{\sigma\sqrt{t-s}} \star (u(s)(|\nabla f(s)| - |\nabla g(s)|))\|_{W^{\epsilon, r^*}} ds \leq \quad (8b)$$

$$C_1 K \left(\int_0^t \|u(s)\|_{L^r}^p s^{p/2} \|f(s) - g(s)\|_{W^{1, r^*}}^p ds \right)^{1/p}$$

$$\int_0^t \|\eta_{\sigma\sqrt{t-s}} \star (u(s)^T \nabla f(s))\|_{W^{\epsilon, r^*}} ds \leq \quad (8c)$$

$$C_0 C_V K \left(\int_0^t \|v(s)\|_{\mathcal{V}}^p s^{p/2} \|f(s) - g(s)\|_{W^{1, r^*}}^p ds \right)^{1/p}$$

Corollary 2. *The mapping Ψ maps P_T into itself. Moreover, given $f, g \in P_T$, one has*

$$\|\Psi_0\|_{P_T} \leq C_0 \|f_0\|_{L^{r^*}} \quad (9a)$$

$$\|\Psi_I(f) - \Psi_I(g)\|_{P_T} \leq 2C_0 C_I T \|f - g\|_{P_T} \quad (9b)$$

$$\|\Psi_u(f) - \Psi_u(g)\|_{P_T} \leq C_1 K \|f - g\|_{P_T} \left(\int_0^T \|u(s)\|_{L^r}^p ds \right)^{1/p} \quad (9c)$$

$$\|\Psi_v(f)\|_{P_T} \leq C_0 C_V K \|f\|_{P_T} \left(\int_0^T \|v(s)\|_V^p ds \right)^{1/p} \quad (9d)$$

Proof of Lemma 3 and Corollary 2. Take $\epsilon \in \{0, 1\}$. Using Eq. (5a), we have $\Psi_0(t) = \eta_{\sigma\sqrt{t}} \star f_0 \in W^{\epsilon, r^*}$ with

$$\|\Psi_0(t)\|_{W^{\epsilon, r^*}} \leq C_0 t^{-\epsilon/2} \|f_0\|_{L^{r^*}},$$

which proves Eq. (9a).

Switching to Ψ_I , we have, for all $s \in [0, T]$,

$$|I(f(s)) - I(g(s))| \leq C_I |f(s) - g(s)|$$

so that $I(f(s)) - I(g(s)) \in L^{r^*}$ and, using Eq. (5a) again, $\eta_{\sigma\sqrt{t-s}} \star (I(f(s)) - I(g(s))) \in W^{\epsilon, r^*}$ with

$$\begin{aligned} \|\eta_{\sigma\sqrt{t-s}} \star (I(f(s)) - I(g(s)))\|_{W^{\epsilon, r^*}} &\leq C_0 (t-s)^{-\epsilon/2} \|I(f(s)) - I(g(s))\|_{L^{r^*}} \\ &\leq C_0 C_I (t-s)^{-\epsilon/2} \|f(s) - g(s)\|_{L^{r^*}}. \end{aligned}$$

This shows that

$$\begin{aligned} \|\Psi_I(f(t)) - \Psi_I(g(t))\|_{W^{\epsilon, r^*}} &\leq \int_0^t \|\eta_{\sigma\sqrt{t-s}} \star (I(f(s)) - I(g(s)))\|_{W^{\epsilon, r^*}} ds \\ &\leq C_0 C_I \int_0^t (t-s)^{-\epsilon/2} \|f(s) - g(s)\|_{L^{r^*}} ds, \end{aligned}$$

which proves Eq. (8a), and Eq. (9b) is derived from $\|f(s) - g(s)\|_{L^{r^*}} \leq \|f - g\|_{P_T}$ and

$$\int_0^t (t-s)^{-\epsilon/2} = t^{1-\epsilon/2} / (1-\epsilon/2).$$

Switching to Ψ_u , we have, for almost all $s \in [0, T]$, $u(s)|\nabla f(s)| \in L^1$ with

$$\|u(s)|\nabla f(s)\|_{L^1} \leq \|u(s)\|_{L^r} \|f(s)\|_{W^{1, r^*}}.$$

It follows from Eq. (5b) that

$$\eta_{\sigma\sqrt{t-s}} \star (u(s)(|\nabla f(s)| - |\nabla g(s)|)) \in W^{\epsilon, r^*}$$

with

$$\begin{aligned} \|\eta_{\sigma\sqrt{t-s}} \star (u(s)(|\nabla f(s)| - |\nabla g(s)|))\|_{W^{\epsilon, r^*}} &\leq C_1 (t-s)^{-\epsilon/2-\gamma_1} \|u(s)(|\nabla f(s)| - |\nabla g(s)|)\|_{L^1} \\ &\leq C_1 (t-s)^{-\epsilon/2-\gamma_1} \|u(s)(|\nabla f(s) - \nabla g(s)|)\|_{L^1} \\ &\leq C_1 (t-s)^{-\epsilon/2-\gamma_1} \|u(s)\|_{L^r} \|f(s) - g(s)\|_{W^{1, r^*}} \end{aligned}$$

It follows that

$$\begin{aligned}
\|\Psi_u(f)(t) - \Psi_u(g)(t)\|_{W^{\epsilon, r^*}} &\leq C_1 \int_0^t (t-s)^{-\epsilon/2 - \gamma_1} s^{-1/2} \|u(s)\|_{L^r} s^{1/2} \|f(s) - g(s)\|_{W^{1, r^*}} ds \\
&\leq C_1 \phi(t, \epsilon/2 + \gamma_1) \left(\int_0^t \|u(s)\|_{L^r}^p s^{p/2} \|f(s) - g(s)\|_{W^{1, r^*}}^p ds \right)^{1/p} \\
&\leq C_1 K \left(\int_0^t \|u(s)\|_{L^r}^p s^{p/2} \|f(s) - g(s)\|_{W^{1, r^*}}^p ds \right)^{1/p},
\end{aligned}$$

which yields Eq. (8b), and Eq. (9c) is a consequence of $s^{1/2} \|f(s) - g(s)\|_{W^{1, r^*}} \leq \|f - g\|_{P_T}$.

Similarly, for almost all $s \in [0, T]$, we have $v(s)^T \nabla f(s) \in L^{r^*}$ with

$$\|v(s)^T \nabla f(s)\|_{L^{r^*}} \leq \|v(s)\|_{C^0} \|f(s)\|_{W^{1, r^*}} \leq C_V \|v(s)\|_V \|f(s)\|_{W^{1, r^*}}.$$

Using Eq. (5a), we get

$$\eta_{\sigma\sqrt{t-s}} \star (v(s)^T \nabla f(s)) \in W^{\epsilon, r^*}$$

with

$$\|\eta_{\sigma\sqrt{t-s}} \star (v(s)^T \nabla f(s))\|_{W^{\epsilon, r^*}} \leq C_0 C_V \|v(s)\|_V (t-s)^{-\epsilon/2} s^{-1/2} s^{1/2} \|f(s)\|_{W^{1, r^*}}.$$

Finally,

$$\begin{aligned}
\|\Psi_v(f)(t)\|_{W^{\epsilon/2, r^*}} &\leq C_0 C_V \phi(t, \epsilon/2) \left(\int_0^t \|v(s)\|_V^p s^{p/2} \|f(s)\|_{W^{1, r^*}}^p ds \right)^{1/p} \\
&\leq C_0 C_V K \left(\int_0^t \|v(s)\|_V^p s^{p/2} \|f(s)\|_{W^{1, r^*}}^p ds \right)^{1/p},
\end{aligned}$$

which gives Eqs. (8c) and (9d).

If $f \in P_T$, these equations (taking $g = 0$) imply that $\sup_{t \in (0, T]} t^\epsilon \|\Psi(f)(t)\|_{W^{1, r^*}} < \infty$. Obviously, $\Psi(f) \in C^0((0, T], W^{\epsilon, r^*})$. But Eqs. (9b) to (9d) show that $\Psi(f)(t)$ has the same limit (in L^{r^*}) as $\eta_{\sigma\sqrt{t}} \star f_0$ when $t \rightarrow 0$, which is equal to f_0 from standard properties of mollifiers, showing that $\Psi(f) \in C^0([0, T], L^{r^*})$. \square

Well defined contraction

A direct consequence of Corollary 2 is that, if T is small enough, such that, say,

$$2C_0 C_I T + C_2 K \left(\int_0^T \|u(s)\|_{L^r}^p ds \right)^{1/p} + C_0 C_V K \left(\int_0^T \|v(s)\|_V^p ds \right)^{1/p} < \frac{1}{2} \quad (10)$$

then Ψ is a contraction on P_T . Choosing such a T , we obtain the fact that there is a unique solution to Eq. (6) in P_T .

Arbitrary integral solution is element of path space

We show that if a function $f \in C^0([0, T'], L^{r^*}) \cap C^0((0, T'], W^{1, r^*})$ with $0 < T \leq T' \leq 1$ is such that

$$f(t) = \eta_{\sigma\sqrt{t}} \star f_0 + \int_0^t \eta_{\sigma\sqrt{t-s}} \star (I(f(s)) + u(s)|\nabla f(s)| - v^T(s)\nabla f(s)) ds$$

then $f|_{[0, T]} \in P_T$, which implies that the function f is the unique fixed point of $\Psi : P_T \rightarrow P_T$. This boils down to showing that $\sqrt{t} \|f(t)\|_{W^{1, r^*}}$ remains bounded when $t \rightarrow 0$.

Let $A_t = \max_{0 < s \leq t} (\sqrt{s} \|f(s)\|_{W^{1,r^*}})$. Using Eq. (9a) and Eqs. (8a) to (8c), we get, for $0 \leq s \leq t \leq T$: $\sqrt{s} \|\Psi_0(s)\|_{W^{1,r^*}} \leq C_0 \|f_0\|_{L^{r^*}}$ and

$$\begin{aligned} \sqrt{s} \|\Psi_I(f)(s)\|_{W^{1,r^*}} &\leq C_0 C_I \sqrt{s} \left(\int_0^s (s-\tilde{s})^{-1/2} \tilde{s}^{-1/2} d\tilde{s} \right) A_s = C_0 C_I \sqrt{s} \Gamma(1/2)^2 A_s \\ \sqrt{s} \|\Psi_u(f)(s)\|_{W^{1,r^*}} &\leq C_1 K \left(\int_0^s \|u(\tilde{s})\|_{L^r}^p d\tilde{s} \right)^{1/p} A_s \\ \sqrt{s} \|\Psi_v(f)(s)\|_{W^{1,r^*}} &\leq C_V K \left(\int_0^s \|v(\tilde{s})\|_V^p d\tilde{s} \right)^{1/p} A_s \end{aligned}$$

Since $f(t) = \Psi(f)(t) = \Psi_0 + \Psi_I(f)(t) + \Psi_u(f)(t) - \Psi_v(f)(t)$, we get (taking the supremum over $s \leq t$)

$$A_t \leq C_0 \|f_0\|_{L^{r^*}} + \left(C_0 C_I \Gamma(1/2)^2 \sqrt{t} + C_1 K \left(\int_0^t \|u(s)\|_{L^r}^p ds \right)^{1/p} + C_V K \left(\int_0^t \|v(s)\|_V^p ds \right)^{1/p} \right) A_t.$$

Taking t_0 small enough so that

$$C_0 C_I \Gamma(1/2)^2 \sqrt{t_0} + C_1 K \left(\int_0^{t_0} \|u(s)\|_{L^r}^p ds \right)^{1/p} + C_V K \left(\int_0^{t_0} \|v(s)\|_V^p ds \right)^{1/p} \leq \frac{1}{2}$$

we get $A_t \leq 2C_0 \|f_0\|_{L^{r^*}}$ for all $t \leq t_0$, showing that $f \in P_T$. □

Global existence

Proof of Theorem 1. Remark that in the previous proof, for any $f_0 \in L^{r^*}$, $u \in \mathcal{U}$, $v \in \mathcal{V}$ the short time existence of a solution to the integral equation depended on picking T such that Eq. (10) is satisfied. Taking the p th power of this equation, and using the inequality $a + b \leq 2^{1/p^*} (|a|^p + |b|^p)$, this equation is satisfied as soon as

$$h(T) := CT + C \int_0^T \|u(s)\|_{L^r}^p ds + C \int_0^T \|v(s)\|_V^p ds \leq \frac{1}{2},$$

with $C = \max(2C_0 C_I, 2^{1/p^*} C_1 K, 2^{1/p^*} C_0 C_V K)$. Since h is continuous in T over $[0, 1]$, there exists (by uniform continuity) a partition $0 = t_0 < t_1 < \dots < t_N = 1$ with fixed mesh size $\Delta t = t_2 - t_1$ on $[0, 1]$ so that for each $i = 0, \dots, N-1$ we have $|h(t_{i+1}) - h(t_i)| \leq 1/2$, i.e.,

$$C \Delta t + C \int_{t_i}^{t_{i+1}} \|u(s)\|_{L^r}^p ds + C \int_{t_i}^{t_{i+1}} \|v(s)\|_V^p ds < \frac{1}{2}. \quad (11)$$

We define the functions $u_i \in \mathcal{U}$, $v_i \in \mathcal{V}$ given for each $i = 0, \dots, N-1$ by

$$\begin{aligned} u_i(t) &= u(t + t_i), \quad t \in [0, \Delta t], \quad u_i(t) = 0, \quad t > \Delta t, \\ v_i(t) &= v(t + t_i), \quad t \in [0, \Delta t], \quad v_i(t) = 0, \quad t > \Delta t. \end{aligned}$$

Given Equation 11 and the fact that

$$\int_{t_i}^{t_{i+1}} \|u(s)\|_{L^r}^p + \|v(s)\|_V^p ds = \int_0^{\Delta t} \|u_i(s)\|_{L^r}^p + \|v_i(s)\|_V^p ds$$

for each i , then each u_i, v_i emit a local integral solution for any given initial data inside of L^{r^*} . So let f^1 denote the unique solution to the integral equation using u_0, v_0, f_0 . We then solve the integral equation

$N - 1$ times iteratively for each $i = 1, \dots, N - 1$. That is, we define f^{i+1} as the short time solution of the integral equation using u_i, v_i, f_i . Then define $f \in C^0([0, 1], L^{r^*}(\mathbb{R}^d)) \cap C^0((0, 1], W^{1, r^*}(\mathbb{R}^d))$ by

$$f(t) = f^i(t - t_i), t \in [t_{i-1}, t_i], i = 1, \dots, N.$$

By definition for $t \in [t_i, t_{i+1}]$, this f satisfies the condition that

$$\begin{aligned} f(t) &= \eta_{\sigma\sqrt{t-t_i}} \star f^i(\Delta t) + \int_{t_i}^{t_{i+1}} \eta_{\sigma\sqrt{t-s}} \star (I(f^{i+1}(s)) + u_i(s)|\nabla f^{i+1}(s)| - v_i(s)^T \nabla f^{i+1}(s)) ds \\ &= \eta_{\sigma\sqrt{t}} \star f(t) + \int_0^t \eta_{\sigma\sqrt{t-s}} \star (I(f(s)) + u(s)|\nabla f(s)| - v(s)^T \nabla f(s)) ds, \end{aligned}$$

which can be shown by using the following iteration, convolution properties of Gaussians, and the definitions of u_i, v_i

$$f^i(\Delta t) = \eta_{\sigma\sqrt{\Delta t}} \star f^{i-1}(\Delta t) + \int_0^{\Delta t} \eta_{\sigma\sqrt{\Delta t-s}} \star (I(f^i(s)) + u_{i-1}(s)|\nabla f^i(s)| - v_{i-1}(s)^T \nabla f^i(s)) ds.$$

This function f is the only function that satisfies this global integral equation since at each time t we have $f(t) = f^i(t - t_i)$ where $f^i(t - t_i)$ uniquely solves the local integral equation. Moreover

$$\begin{aligned} \max \left(\sup_{t \in [0, 1]} \|f(t)\|_{L^{r^*}}, \sup_{t \in (0, 1]} \sqrt{t} \|f(t)\|_{W^{1, r^*}} \right) \leq \\ \max_{i=0, \dots, N-1} \left(\max \left(\sup_{t \in [t_i, t_{i+1}]} \|f^{i+1}(t)\|_{L^{r^*}}, \sup_{t \in (t_i, t_{i+1}]} \sqrt{t} \|f^{i+1}(t)\|_{W^{1, r^*}} \right) \right) < \infty. \end{aligned}$$

And, lastly, $\lim_{t \rightarrow 0} f(t) = f_0$ almost everywhere in \mathbb{R}^d as

$$\lim_{t \rightarrow 0} \|f(t) - f_0\|_{L^{r^*}} = \lim_{t \rightarrow 0} \|f^1(t) - f_0\|_{L^{r^*}} = 0.$$

□

5 A discrete-time optimal control problem

5.1 Discrete-time evolution

Let T be a positive integer and let $\Delta t = \frac{1}{T}$. We discretize $[0, 1]$ uniformly into the $T + 1$ -tuple given by $t_0 = 0, t_1 = \Delta t, t_2 = 2\Delta t, \dots, t_T = T\Delta t = 1$. Let $p \in (2, \infty)$, and $r \in \left(\frac{dp}{p-2}, \infty\right)$. We define $P = C([0, 1], L^{r^*}) \cap C([0, 1], W^{1, r^*})$ and

$$Q_T = \{f : f : \{1, \dots, T\} \rightarrow C_0^1\},$$

where $\frac{1}{r} + \frac{1}{r^*} = 1$ and identify elements of Q_T as $T + 1$ -tuples with $f_0 \in L^{r^*}$ and $f_i \in C_0^1$ for $i = 1, \dots, T$. Define the subspaces \mathcal{U}_T of \mathcal{U} and \mathcal{V}_T of \mathcal{V} by

$$\mathcal{U}_T = \{u \in \mathcal{U} : u_{[t_i, t_{i+1}]} = u_i, u_i \in L^r \forall i = 1, \dots, T - 1, u_{[t_0, t_1]} = 0\}.$$

$$\mathcal{V}_T = \{v \in \mathcal{V} : v_{[t_i, t_{i+1}]} = v_i, v_i \in V \forall i = 1, \dots, T - 1, v_{[t_0, t_1]} = 0\}.$$

So by definition, the r -th, 2-th powers of the norms of $u, v \in \mathcal{U}_{\Delta t}, \mathcal{V}_{\Delta t}$ can be written as a finite sum

$$\|u\|_{\mathcal{U}}^r = \int_0^1 \|u(t)\|_{\mathcal{U}}^r dt = \sum_{t=1}^{T-1} \|u_i\|_{L^p}^r \Delta t, \quad \|v\|_V^2 = \int_0^1 \|v(t)\|_V^2 dt = \sum_{t=1}^{T-1} \|v_i\|_V^2 \Delta t,$$

where $u_i = u_{[t_i, t_{i+1})}, v_i = v_{[t_i, t_{i+1})}$ for all $i = 1, \dots, T-1$. So we write u_i, v_i to refer to the i -th entry of an element of $\mathcal{U}_T, \mathcal{V}_T$ and regard its elements as $T-1$ -tuples in L^r and V . We pick some small constant $\psi > 0$, and define

$$\chi(z) = \sqrt{|z|^2 + \psi^2}$$

as a smooth approximation of $z \mapsto |z|$. We note that the gradient of χ is $\nabla \chi(z) = \frac{z}{\sqrt{|z|^2 + \psi^2}}$, with $|\nabla \chi(z)| \leq 1$ and its Hessian is

$$\nabla^2 \chi = \frac{(|z|^2 + \psi^2)I_{\mathbb{R}^d} - zz^T}{(|z|^2 + \psi^2)^{3/2}} \geq \frac{I_{\mathbb{R}^d}}{\psi}$$

where $I_{\mathbb{R}^d}$ is the d -dimensional identity matrix and the inequality is meant for the usual partial order between symmetric matrices (positive semi-definite difference). Since $\chi(0) = 0$, we have $\chi(z) \leq |z|$ for all z .

Let $\tau = \sigma\sqrt{\Delta t}$. By Lemma 2, $h \mapsto \eta_\tau \star h$ is a bounded linear mapping from any L^q to C_0^1 , and from C_0^0 to C_0^1 . Define $G : C_0^1 \times L^r \times V \rightarrow C_0^1$ by

$$G(f', u', v') = \eta_\tau \star f' + \eta_\tau \star (\chi(\nabla f')u' - \nabla f'^T v' + I(f')). \quad (12)$$

We verify that G is indeed a bounded operator in the following lemma and will end this section by proving G is Fréchet differentiable.

Lemma 4. *We claim G in Eq. (12) is a bounded operator. That is, for $f' \in C_0^1$, $u' \in L^r$, and $v' \in V$ and for some constant $C' > 0$ we have*

$$\|G(f', u', v')\|_{C^1} \leq C' \|f'\|_{C^1} (1 + \|u'\|_{L^r} + \|v'\|_V) \quad (13)$$

Proof. Using Lemma 2, $f' \mapsto \eta_\tau \star f'$ is bounded and linear from C_0^1 into C_0^1 . We have, for some constant C ,

$$\|\eta_\tau \star (\chi(\nabla f')u')\|_{C^1} \leq C \|\chi(\nabla f')u'\|_{L^r}.$$

Moreover

$$\|\chi(\nabla f')u'\|_{L^r} \leq \|\chi(\nabla f')\|_{C^0} \|u'\|_{L^r} \leq \|f'\|_{C^1} \|u'\|_{L^r}. \quad (14)$$

For the convective term, we have, for some constant, C ,

$$\|\eta_\tau \star (\nabla f'^T v')\|_{C^1} \leq C \|\nabla f'^T v'\|_{C^0} \leq C \|f'\|_{C^1} \|v'\|_{C^0} \leq C_V C \|f'\|_{C^1} \|v'\|_V. \quad (15)$$

Lastly the reaction term is bounded as

$$\|\eta_\tau \star I(f')\|_{C^1} \leq C \|I(f')\|_{C^0} \leq C_0 C_I \|f'\|_{C^0}.$$

As we add the terms above, we can bound $\|G(f', u')\|_{C^1}$ as claimed. \square

We define a discrete-time evolution as follows.

Proposition 1. *Let $f_0 \in L^{r^*}$, $u \in \mathcal{U}_T$, and $v \in \mathcal{V}_T$. Let $f_1 = \eta_\tau \star f_0$ and for each $i = 1, \dots, T-1$ define*

$$f_{i+1} = G(f_i, u_i, v_i).$$

Then $f_{1:T} \in Q_T$, i.e., $f_i \in C_0^1$ for every $i = 1, \dots, T$.

Proof. This is clear, given the previous lemma, since $f_1 = \eta_\tau \star f_0 \in C_0^1$. \square

One can show that, for given $f_0 \in Q$ and $u \in \mathcal{U}_T$, $v \in \mathcal{V}_T$, the function f defined in the proposition above has the property that

$$f_{k+1} = \eta_{\tau\sqrt{k+1}} \star f_0 + \sum_{j=1}^k \eta_{\tau} \star G(f_j, u_j, v_j) \Delta t, \quad \forall k \geq 2. \quad (16)$$

Moreover, one can define a $f \in P$ such that $f(t_k) = f_k$ for every $k = 0, 1, \dots, T$ by defining for $k = 0, \dots, T-1$

$$f(t_k + s) = \eta_{\sigma\sqrt{s}} \star f_k + \eta_{\sigma\sqrt{s}} \star G(f_k, u_k, v_k) s.$$

5.2 Variational derivatives of the discrete evolution equation

In this section we prove the following theorem.

Theorem 3. *The function $G : C_0^1 \times L^r \times V \rightarrow C_0^1$ in Eq. (12) is continuously differentiable in a Fréchet sense. One has*

$$\partial_u G(f, u, v) \delta u = \eta_{\tau} \star (\chi(\nabla f) \delta u) \quad (17a)$$

$$\partial_v G(f, u, v) \delta v = -\eta_{\tau} \star (\nabla f^T \delta v) \quad (17b)$$

$$\partial_f G(f, u, v) \delta f = \eta_{\tau} \star \delta f + \eta_{\tau} \star (u \nabla \chi(\nabla f)^T \nabla \delta f) - v^T \nabla \delta f + I'(f) \delta f \quad (17c)$$

Proof. From Eqs. (14) and (15), G is linear and bounded with respect to u and v , so that one only needs to consider its differentiability in f

The mapping $f \mapsto \eta_{\tau} \star f$ is a bounded linear mapping from C_0^1 to itself, hence differentiable. The same is true, using Eq. (15), for $f \mapsto \eta_{\tau} \star (v^T \nabla f)$ if $v \in V$. Let C'_I be an upper-bound of both first and second derivatives of I . We have

$$|I(f+h) - I(f) - I'(f)h| \leq C'_I |h|^2,$$

Then

$$\|\eta_{\tau} \star (I(f+h) - I(f) - I'(f)h)\|_{C^1} \leq C'_I \|h\|_{C^1}^2.$$

showing that $f \mapsto \eta_{\tau} \star I(f)$ is differentiable, with differential $h \mapsto \eta_{\tau} \star (I'(f)h)$.

Finally, for $u \in L^r$, we have

$$\|\chi(\nabla f + \nabla h) - \chi(\nabla f) - \nabla \chi(\nabla f)^T \nabla h\|_{C^0} \leq \frac{|\nabla h|^2}{\psi}$$

and this implies that, for some constant C ,

$$\|\eta_{\tau} \star (\chi(\nabla f + \nabla h) - \chi(\nabla f) - \nabla \chi(\nabla f)^T \nabla h)\|_{C^1} \leq \frac{C}{\psi} \|u\|_{L^r} \|h\|_{C^1}^2.$$

□

We will need below the expressions of the the adjoints of the partial derivatives of G , where $\partial_u G^*$, $\partial_v G^*$, $\partial_f G^*$ and defined on $(C_0^1)^*$ and take values, respectively, in L^{r^*} , V^* and $(C_0^1)^*$. For a Banach space B , let the pairing of a dual vector $\lambda \in B^*$ and vector $v \in B$ be denoted by $(\lambda | v)$. If $\lambda \in (C_0^1)^*$, we will use the notation

$$(\lambda \star \eta_{\tau} | h) = (\lambda | \eta_{\tau} \star h)$$

and $\lambda \star \eta_{\tau}$ belongs to $(C_0^1)^*$ and to L^{q^*} for any $q > 1$. From eqs. (17a-17c), we get (letting $\nabla \cdot$ denote the divergence operator),

$$\partial_u G(f, u, v)^* \lambda = \chi(\nabla f) (\lambda \star \eta_{\tau}) \quad (18a)$$

$$\partial_v G(f, u, v)^* \lambda = -\nabla f (\lambda \star \eta_{\tau}) \quad (18b)$$

$$\partial_f G(f, u, v)^* \lambda = (1 + I'(f)) \lambda \star \eta_{\tau} - \nabla \cdot ((u \nabla \chi(\nabla f) - v) \lambda \star \eta_{\tau}). \quad (18c)$$

5.3 Characterization of Minimizers

We follow Appendix D.4 of [66] and Chapters 4 and 7 of [64] to formulate a Lagrange multiplier method, which can be used to derive a discrete-time version of Pontryagin's Maximum Principle. For a continuous-time maximum principle, see Appendix D.3.1 of [66] and Chapters 4 and 7 of [64].

Proposition 2. *Let $f_0 \in L^{r^*}$ and let $U : C_0^1 \rightarrow \mathbb{R}$ be continuously Fréchet differentiable, and bounded from below. We seek to minimize $E : Q_T \times \mathcal{U}_T \times \mathcal{V}_T \rightarrow \mathbb{R}$ given by*

$$E(f, u, v) = \Delta t \sum_{k=1}^{T-1} (C_{\text{top}} \|u_k\|_{L^r}^p + \|v_k\|_V^p) + U(f_T)$$

subject to the constraint that $f = f(f_0, u, v)$ where

$$f_{k+1} = G(f_k, u_k, v_k), \quad k = 1, \dots, T-1, \quad f_1 = \eta_\tau \star f_0.$$

If (f, u, v) is a minimizer of E subject to this constraint then there is a $\lambda : \{1, \dots, T\} \rightarrow (C_0^1)^*$ such that (f, u, v, λ) are critical points of the Lagrangian

$$\begin{aligned} \mathcal{L}(f, u, v, \lambda) = & \sum_{k=1}^{T-1} (C_{\text{top}} \|u_k\|_{L^r}^p + \|v_k\|_V^p) + U(f_T) + \sum_{k=2}^T (\lambda_k | f_k - G(f_{k-1}, u_{k-1}, v_{k-1})) \\ & + (\lambda_1 | f_1 - \eta_{\sigma\sqrt{\Delta t}} \star f_0) \end{aligned} \quad (19)$$

Proof. The mapping $u \mapsto \|u\|_{L^r}^p$ is differentiable on L^r with differential $p\|u\|_{L^r}^{p-r} |u|^{r-1} \text{sign}(u)$ and $v \mapsto \|v\|_V^p$ is differentiable on V with gradient $p\|v\|_V^{p-2} v$. Since U is assumed to be differentiable, we can conclude that E is differentiable.

The constraints are $\Gamma(f, u, v) = 0$ where $\Gamma = (\Gamma_1, \dots, \Gamma_T)$ with

$$\Gamma_i((f, u, v)) = f_i - G(f_{i-1}, u_{i-1}, v_{i-1}), \quad i = 2, \dots, T; \quad \Gamma_1((f, u)) = f_1 - \eta_\tau \star f_0.$$

Theorem 3 states that each Γ_i is differentiable, and, since Γ is defined through a triangular system, one gets the fact that $\partial_f \Gamma$ is onto. These properties are sufficient for the Lagrange multipliers theorem, as stated in Proposition 2, to hold. \square

We then have the following discrete-time evolution equation for λ below. (Compare with (1.8), pp 131 of [64] and D.20, pp of [66].)

Corollary 3. *Critical points of the Lagrangian (19) in Proposition 2 are such that the following discrete time evolution holds:*

$$\lambda_T = dU(f_T), \quad \lambda_k = -\partial_f G(f_k, u_k, v_k)^* \lambda_{k+1} \quad k = 1, \dots, T-1 \quad (20)$$

Moreover, if we set $\tilde{E} : \mathcal{U}_T \times \mathcal{V}_T \rightarrow \mathbb{R}$ as $\tilde{E}((u, v)) = E(f(f_0, (u, v)), (u, v))$, then (setting $f = f(f_0, (u, v))$) we have

$$\partial_u \tilde{E}((u, v))_k = \partial_u \mathcal{L}(f, u, v, \lambda) = \Delta t C_{\text{top}} p \|u_k\|_{L^r}^{p-r} \cdot u_k^{r-1} - \partial_u G(f_k, u_k, v_k)^* \lambda_{k+1}, \quad (21)$$

$$\partial_v \tilde{E}((u, v))_k = \partial_v \mathcal{L}(f, u, v, \lambda) = \Delta t p \|v_k\|_V^{p-2} \cdot v_k - \partial_v G(f_k, u_k, v_k)^* \lambda_{k+1}, \quad (22)$$

for $k = 1, \dots, T-1$.

We call the problem described in Proposition 2 a soft end point minimization optimal control problem. We use the discrete evolution of λ in Eq. (20) in the next numerical results section to numerically find optimal u, v given an initial guess—this is called an adjoint shooting method.

6 Numerical simulation

In this section we show some two-dimensional simulations of the spatially discretized version of the above optimal control problem.

6.1 Maximum bounded principle enforcing time step

One valuable property to be preserved by discretizations of Allen-Cahn equations is the maximum bounded principle (MBP), that is, if $-\infty < a = \min_{x \in \mathbb{R}^d} (f_0)$ and $b = \max_{x \in \mathbb{R}^d} (f_0) < \infty$, then $a \leq f(t, x) \leq b$ for all $t \in [0, 1]$ and $x \in \mathbb{R}^d$. This is a property enjoyed by the convective Allen-Cahn equation for $u = 0$, [49] gives an example MBP preserving discretization scheme for this case. The MBP is also enjoyed by a variety of semi-linear parabolic equations; an example of an MBP-preserving discretization scheme is provided by [19].

We modify the discrete time evolution presented in the previous section to artificially enforce this property.

First we present a slightly modify the discrete time evolution, so that we can use properties of the derivatives of convolution. We first remark that the discrete time step $f_{k+1} = G(f_k, u_k, v_k)$ for $k = 1, \dots, T-1$ and $f_1 = \eta_{\sigma\sqrt{\tau}} \star f_0$ is equal to (still letting $\tau = \sigma\sqrt{\Delta t}$)

$$F_{k+1} = (\eta_\tau \star F_k) + \Delta t (\chi(|\nabla \eta_\tau \star F_k|)u_k - \nabla \eta_\tau \star F_k^T v_k + I(\eta_\tau \star F_k)) \quad (23)$$

for $k = 1, \dots, T-1$ and $F_0 = f_0$. The iterations are related by $f_k = \eta_\tau \star F_k$ for all $k = 0, \dots, T$. We have used the fact that f_k , for $k \geq 1$, is in C_0^1 so $\eta_\tau \star \nabla f_k = \nabla \eta_\tau \star f_k$, and χ is the same as before.

Our spatial discretization in the next section will evaluate $\nabla \eta_\tau$ over a matrix of points. But we approximate this forward Euler time step for F_{k+1} in the following way, which enforces the maximum bounded principle; heuristically, we write $F_{k+1} = \tilde{F}_k + \Delta t V_k$. Suppose $a = \inf_{\mathbb{R}^d} (f_0) > -\infty$ and $b = \sup_{\mathbb{R}^d} (f_0) < \infty$. Then we pick a C^2 , analytic, monotonic increasing function $g : [a, b] \rightarrow \mathbb{R}$ and consider the following scheme

$$\begin{aligned} F_{k+1} &= g^{-1}(g(f_k) + \Delta t g'(f_k)V_k), \\ V_k &= \chi(|\nabla f_k|) - \nabla f_k^T v_k + I(f_k) \\ f_k &= \eta_\tau \star F_k. \end{aligned}$$

We use a Taylor expansion and the inverse function theorem to show that the update rule is at least as accurate as a first order forward Euler scheme as

$$g^{-1}(g(f_k) + \Delta t g'(f_k)V_k) \approx f_k + \Delta t V_k + O(\Delta t).$$

And by construction, $a \leq F_{k+1}(x), f_{k+1}(x) \leq b$ for all $x \in \mathbb{R}^d$. Note that we do not show that the continuous-time mild solution obeys the maximum bounded principle, but it is a reasonable conjecture and that we aim to tackle in a future work. So, the Lagrangian we will use is

$$\mathcal{L}(F, u, v, \lambda) = \Delta t \sum_{k=1}^{T-1} (C_{\text{top}} \|u_k\|_{L^r}^p + \|v_k\|_V^p) + U(\eta_\tau \star F_T) + \sum_{k=1}^{T-1} (\lambda_{k+1} | F_{k+1} - \tilde{G}(F_k, u_k, v_k)) \quad (24)$$

where F_k and V_k are defined above and

$$\tilde{G}(F_k, u_k, v_k) = g^{-1}(g(\eta_\tau \star F_k) + \Delta t g'(\eta_\tau \star F_k)V_k).$$

Remark, there is a $f \in P$ such that $f(t_k) = f_k$ for every $k = 0, 1, \dots, T$. For $k = 0, \dots, T-1$ and $s \in [0, \Delta t]$ it is given by

$$f(t_k + s) = \eta_{\sigma\sqrt{s}} \star g^{-1}(g(f_k) + \tau g'(f_k)V_k)$$

which has the property

$$f(t_k + s) = \eta_{\sigma\sqrt{s}} \star f_k + s \eta_{\sigma\sqrt{s}} \star V_k + o(s).$$

6.2 Spatial discretization in two dimensions

6.2.1 Grid setup, initial and target data

Let $L > 0$, and $N > 0$ be a large odd integer and consider the set of points $(x_i, x_j)_{i,j=1}^N$ where $x_i = -L + \Delta x(i-1)$ and $\Delta x = \frac{2L}{N-1}$ is the mesh parameter. This will be our discretized $[-L, L]^2$. Let $T > 0$ be an integer and consider the set of points $(t_k)_{k=1}^T$ where $t_k = (k-1)\Delta t$ and $\Delta t = \frac{1}{T-1}$. Then for any $V_0, V_1 \subset [-L, L]^2$ we define our initial data f_0 as the $N \times N$ matrix with entries $[f_0]_{ij} = \mathbf{1}_{V_0}((x_i, x_j))$ and our target data f_1 as the $N \times N$ matrix with entries $[f_1]_{ij} = \mathbf{1}_{V_1}((x_i, x_j))$. Moreover, for $\sigma > 0$, $\tau = \sigma\sqrt{\Delta t}$, define the $N \times N$ matrices M and DM by their entries

$$[M]_{ij} = \frac{(\Delta x)^2}{\sqrt{2\pi\tau^2}} \exp\left(-\frac{x_i^2 + x_j^2}{2\tau^2}\right), \quad [DM]_{ij} = -\frac{x_i}{\tau^2} \cdot [M]_{ij}.$$

We discretize the convolution operators and their derivatives by taking the following discrete linear convolutions

$$\eta_\tau \star h \approx M \star h((x_i, x_j)), \quad \partial_{x_1} \eta_\tau \star h \approx DM \star h((x_i, x_j)), \quad \partial_{x_2} \eta_\tau \star h \approx DM^T \star h((x_i, x_j)).$$

6.2.2 Finite Dimensional Subspaces of the Control Spaces

Subspaces of L^r and V are built on the grid above but in different fashions. Define the subspace of simple functions

$$L_N^r = \left\{ u \in L^r : u = \sum_{i,j=1}^N u_{ij} \mathbf{1}_{V_{ij}}, u_{ij} \in \mathbb{R}, \forall 1 \leq i, j \leq N \right\},$$

$$V_{ij} = \{(x, y) : x_i \leq x < x_{i+1}, x_j \leq y < x_{j+1}\}$$

and define the subspace

$$\mathcal{U}_{T,N} = \{u \in \mathcal{U}_T : u(t) \in L_N^r, \forall t \in [0, 1]\}.$$

We denote the elements of $\mathcal{U}_{T,N}$ by their constant coefficients u_{ij}^k where $1 \leq k \leq T$ and $1 \leq i, j \leq N$. Remark that, in this case

$$\|u\|_{\mathcal{U}}^p = \Delta t \sum_{k=1}^T \left((\Delta x)^2 \sum_{i,j=1}^N (u_{ij}^k)^r \right)^{p/r}, \quad \forall u \in \mathcal{U}_{T,N}. \quad (25)$$

The space V of admissible vector fields v is built as a reproducing kernel Hilbert space by selecting a radial kernel function $K : \mathbb{R}^d \times \mathbb{R}^d \rightarrow \mathbb{R}$ (i.e., $K(x, y) = \kappa(|x - y|)$ for some function κ); see [66], Chapter 8. We then select a finite dimensional subspace $V_N \subset V$ defined as the coupled span of kernel functions centered around each point (x_i, x_j) :

$$V_N = [\text{span}(K((\cdot, \cdot), (x_i, x_j)) : i, j = 1, \dots, N)]^2$$

so that the grid points $(x_i, x_j)_{i,j=1}^N$ are collocation points of V_N . So any velocity vector field $v \in V_N$ is written as

$$v(x) = (v^{(1)}(x), v^{(2)}(x)) = \left(\sum_{i,j=1}^N K(x, (x_i, x_j)) m_{i,j}^{(1)}, \sum_{k,l=1}^N K(x, (x_k, x_l)) m_{k,l}^{(2)} \right)$$

where $(m^{(1)}, m^{(2)})$ are the momenta matrices which define the momentum linear functional

$$m = \left(\sum_{i,j=1}^N m_{i,j}^{(1)} \delta_{(x_i, x_j)}, \sum_{k,l=1}^N m_{k,l}^{(2)} \delta_{(x_k, x_l)} \right) \in V_N^*$$

that canonically represents elements of V_N^* . Note that $\delta \in C^1(\mathbb{R}^d, \mathbb{R})^*$ is the dirac delta functional defined by $(\delta_x, \psi) = \psi(x)$ for $\psi \in C^1$. If $m \in V_N^*$ then, using the canonical duality operator $\mathbb{K} : V^* \rightarrow V$, we have $\mathbb{K}m = v$. The norm of $v \in V_N$ is determined by m and a matrix \tilde{K} .

$$\|v\|_V^2 = \sum_{k=1}^2 \left(m^{(k)} |v^{(k)} \right) = \sum_{k=1}^2 \sum_{i,j}^N m_{i,j}^{(k)} v^{(k)}((x_i, x_j)) = \sum_{k=1}^2 \sum_{i,j}^N m_{i,j}^{(k)} \left(\tilde{K} m^{(k)} \right)_{i,j} \quad (26)$$

where

$$[\tilde{K}]_{i,j} = K((x_i, x_j), (0, 0)) = \kappa(|x_i - x_j|).$$

Remark as well that $\|m\|_{V^*}^2 = \|v\|_V^2$. Note that V_N does not have a mesh parameter and is called mesh free, but the grid we chose is called its collocation points.

6.2.3 Evolution Equation

For a given $u \in \mathcal{U}_{T,N}$, $m \in \mathcal{M}_{T,N}$, and initial data function $F_0 \in L^{r^*}$ consider the time discrete, spatially “continuous” scheme

$$\begin{aligned} F(k+1) &= g^{-1}(g(f(k)) + \Delta t g'(f(k))V(k)), \\ V(k) &= \chi(|\nabla f(k)|)u_k - \nabla f(k)^T (\mathbb{K}m(k)) + I(f(k)) \\ f(k) &= \eta_\tau \star F(k). \end{aligned}$$

This scheme defines a $(F(k))_{k=1}^T \in Q_T$. We discretize this scheme spatially by updating N by N matrices rather than functions:

$$\begin{aligned} f(k+1) &= M \star F(k) \\ F(k) &= g^{-1}(g(f(k)) + \Delta t g'(f(k)) \cdot V(k)) \\ V(k) &= u(k) \cdot ((DM \star f(k)) \cdot (DM \star f(k)) + (DM^T \star f(k)) \cdot (DM^T \star f(k)) + \Delta t \epsilon \text{Id})^{1/2} \\ &\quad - v^{(1)}(k) \cdot (DM \star f(k)) - v^{(2)}(k)^k \cdot (DM^T \star f(k)) + I(f(k)) \\ v^{(n)}(k) &= \tilde{K} m^{(n)}(k), \quad n = 1, 2 \end{aligned}$$

where we use $A \cdot B$ to denote entry-wise multiplication of matrices A and B with the same shape and take $\epsilon = 10^{-16}$. This numerical scheme is equivalent to mapping the function $F(k+1)$ to L_N^r through $[F_{ij}(k) = \sum_{i,j=1}^N F(k, (x_i, x_j)) \mathbf{1}_{V_{ij}(k)}(x_i, x_j)]$ at each time step before computing $f(k+1)$. Remark that we avoid finite difference derivatives and directly compute the derivative of η_τ at our grid points within the definitions of M, DM . Within our implementation, we define g as follows. For small $a \geq 0$ and small $\mu > 0$, let $g : [-a, 1+a] \rightarrow \mathbb{R}$ be given by $g(x) = \frac{1}{2} + \mu \log \left(\frac{x+a}{1+a-x} \right)$.

6.2.4 Objective Function

In what follows we view f_T as a function of $f_0 \in L^{r^*}$, $u \in \mathcal{U}_{T,N}$, $m \in \mathcal{M}_{T,N}$ and write $f_T(f_0, u, m)$. We define $E : \mathcal{U}_{T,N} \times \mathcal{M}_{T,N} \rightarrow \mathbb{R}$ by

$$E(u, v) = C_{\text{top}} \|u\|_{\mathcal{U}}^p + \|v(m)\|_V^p + U(f_T(f_0, u, m)),$$

where we use the formulas 25 and 26 to compute the first two terms and $U : W^{1,r^*} \rightarrow \mathbb{R}$ is a C^1 functional that is bounded below by zero. For example, one may take $U(f_T(f_0, u, m))$ as the discretization of $C \|f_T(f_0, u, v) - f_T(f_{\text{target}, v, m})\|_{W^{1,r^*}}^{r^*}$ where $C > 0$ is a large constant.

6.2.5 Gradient of E

To perform gradient descent, one can use a Lagrange multiplier method

$$\mathcal{L}(F, u, m, \lambda) = C_{\text{top}} \|u\|_{\mathcal{U}}^p + \|v(m)\|_{\mathcal{V}}^p + U(\eta_{\sigma\sqrt{t}} \star F_T) + \sum_{k=1}^{T-1} \left(\lambda_{k+1} | F_{k+1} - \tilde{G}(F_k, u^k, m^k) \right) \quad (27)$$

to introduce a discrete costate $\lambda : \{1, \dots, T\} \rightarrow M^{N \times N}$ whose evolution is given by

$$[\lambda(T)]_{ij} = -[\partial_{F(T)} U(f(T))]_{ij} \quad (28)$$

$$\lambda(k) = (\partial_{F(k)} G(k))^* \lambda(k+1), \quad k = 1, \dots, T-1 \quad (29)$$

$$G(k) = g^{-1}(g(M \star F(k)) + g'(M \star F(k))V(k)) \quad (30)$$

The derivatives of our objective function E with respect to u and m are given by

$$[\partial_u E(u, m)(k)]_{ij} = p\Delta t C_{\text{top}} \left((\Delta x)^2 \sum_{l, l'=1}^N (u_{ll'}(k))^r \right)^{(p-r)/r} |u_{ij}(k)|^{r-2} u_{ij}(k) - [(\partial_u G(k))^* \lambda(k)]_{ij}$$

and for each $n = 1, 2$

$$[\partial_{m^{(n)}} E(u, m)(k)]_{ij} = p\Delta t \left(\sum_{l, l'=1}^N m_{ll'}^{(n)}(k) v_{ll'}^{(n)}(k) \right)^{(p-2)/2} (v^{(n)})_{ij}(k) - [(\partial_{m^{(n)}} G(k))^* \lambda(k)]_{ij}$$

where $(v^{(n)})_{ij}(k) = \left(\tilde{K} m^{(n)}(k) \right)_{i,j}$.

6.3 Experimental results

By using a LBFGS method with the definition of $E(u, v)$ and $dE(u, v)$, we performed gradient descent with initial guess $u, v = 0$ using MATLAB. We tested several initial and final images, with different or identical topology. Unless mentioned otherwise, our experiments use $T = 30$, $L = 1$, $N = 150$, $\sigma = 1/10$ and $C_{\text{top}} = 10^8$. These are referred to, below, as default parameters.

6.3.1 Sets of discs

We start with a simple example, in Figure 1, where an original disc shape is transformed into a target that contains two discs. The result of the optimal evolution is provided with a progressive elongation of the disc, creating a neck that breaks to provide two discs. Figure 2 provides an illustration of the relative impact of the topological and advection controls (u and v) when the parameter is changed to 10^6 , 10^8 (same as in Figure 1) and 10^{10} . The diffeomorphic transformation becomes larger, but never changes (as expected) the topology of the original shape.

The images in Figure 2 must be interpreted with some care. Displays in the second column provide the solution at time $t = 1$ of the equation $\partial_t \varphi = v \circ \varphi$. When the effect of the control u on the evolution of f is not negligible, the original image transformed by φ is generally behind the one controlled by u and v together. This is illustrated by the red dots stopping short of the target shapes. The transformation of background points (in blue) completes the description of the function φ and of how it operates on the actual moving shapes. Similarly, the last column in the figure illustrates the overall action of the normal field u had the diffeomorphic transformation been absent. It provides qualitative insights on this part of the process, with, in this case, a combination of horizontal stretching and vertical pinching.

Our second example, in Figs. 3 and 4, transforms three discs into four and conversely. It first illustrates that our process is not symmetric, as the way two components merges is quite different from the way one component splits. One can nonetheless notice similarities between the deforming shapes at time t for the forward process and $1 - t$ for the backward one.

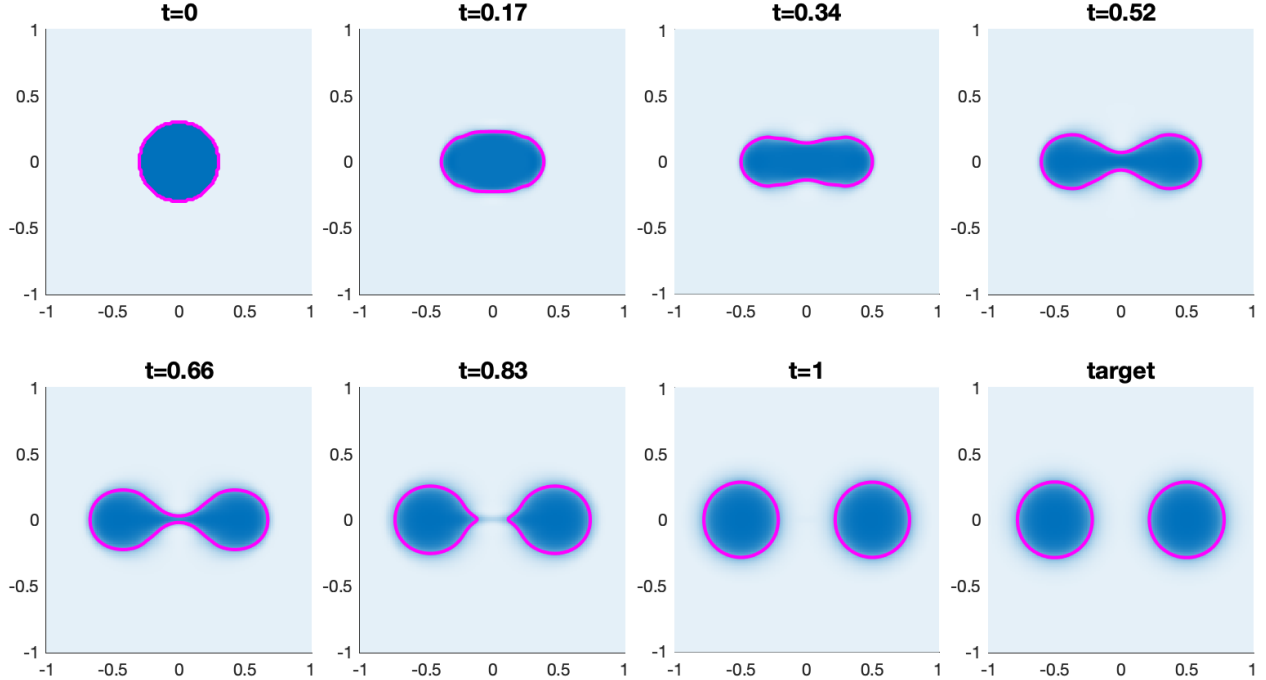


Figure 1: Here our initial shape was the unit disk and the final shape was two unit disks under a Gaussian blur. Presented is the trajectory of the function f (superimposed with its main contour in magenta) at seven time points and the last image is the target image. (Using default parameters.)

6.3.2 Complex Changes of Topology and Geometry

The examples in this section depict shapes based on hand gestures. The first example, in Figure 5, transformed a hand performing an “okay” sign into an open hand. Figure 6 illustrate the respective effects of diffeomorphic and topological changes, where, in this case, most of the motion is operated by the advection, while the normal motion mainly breaks the bridge between the thumb and the index finger.

Figures 7, 8 and 9 compare a hand performing a “vulcan salute” in which the hand is parted between the middle and ring finger and an open hand. Even though the two shapes are topologically equivalent, the trajectories followed by the transformations exhibit significant differences according to the value of the coefficient C_{top} . For $C_{\text{top}} = 10^6$ (Figure 7), an indent is created on the middle finger, leading to a hole positioning itself at the separation between the first two fingers. A similar indent is created in Figure 8, with $C_{\text{top}} = 10^6$, but does not lead to a topological change. The indent almost completely disappears with $C_{\text{top}} = 10^{10}$ (Figure 9).

Our last illustration compares a closed hand with a hand with two raised fingers (Figure 10).

7 Summary

In conclusion, this is a new alignment method that can align any shape’s characteristic function to a target shape’s characteristic function which has undergone mean curvature flow. We prove the existence of solutions given any choice of controls $(u, v) \in \mathcal{U} \times \mathcal{V}$, set up a discrete time soft end point minimization problem. With a Lagrange Multiplier result we characterized minimizers for the discrete time problem, and demonstrate simulations of this approach. Our numerical simulations also enforce the maximum bounded principle. With $(u, v) = (0, 0)$ our numerical simulations demonstrate approximate mean curvature flow. And one can analyze the role of geometric change in shape transformation and topological change by weighing the norms

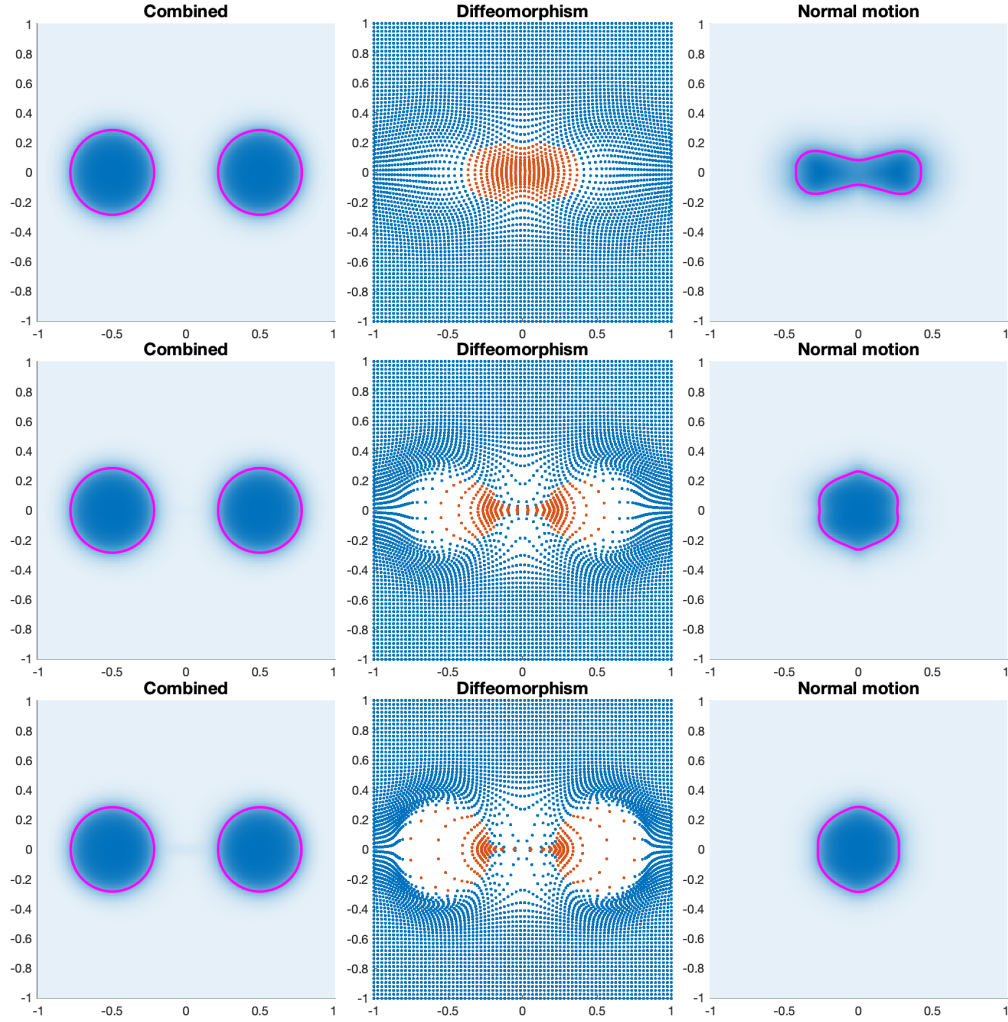


Figure 2: Illustration of the impact of the penalty parameter. The rows correspond, from top to bottom, to $C_{\text{top}} = 10^6$, 10^8 and 10^{10} , using default parameters otherwise. Each row provides, from left to right, the final image ($t = 1$) resulting from the state equation, the diffeomorphism associated to the smooth vector field v (solution to the flow equation at $t = 1$), visualized by applying it to a regular grid, with different colors for connected components of the original image, and the result of only applying the normal motion (setting $v = 0$) in the state equation.

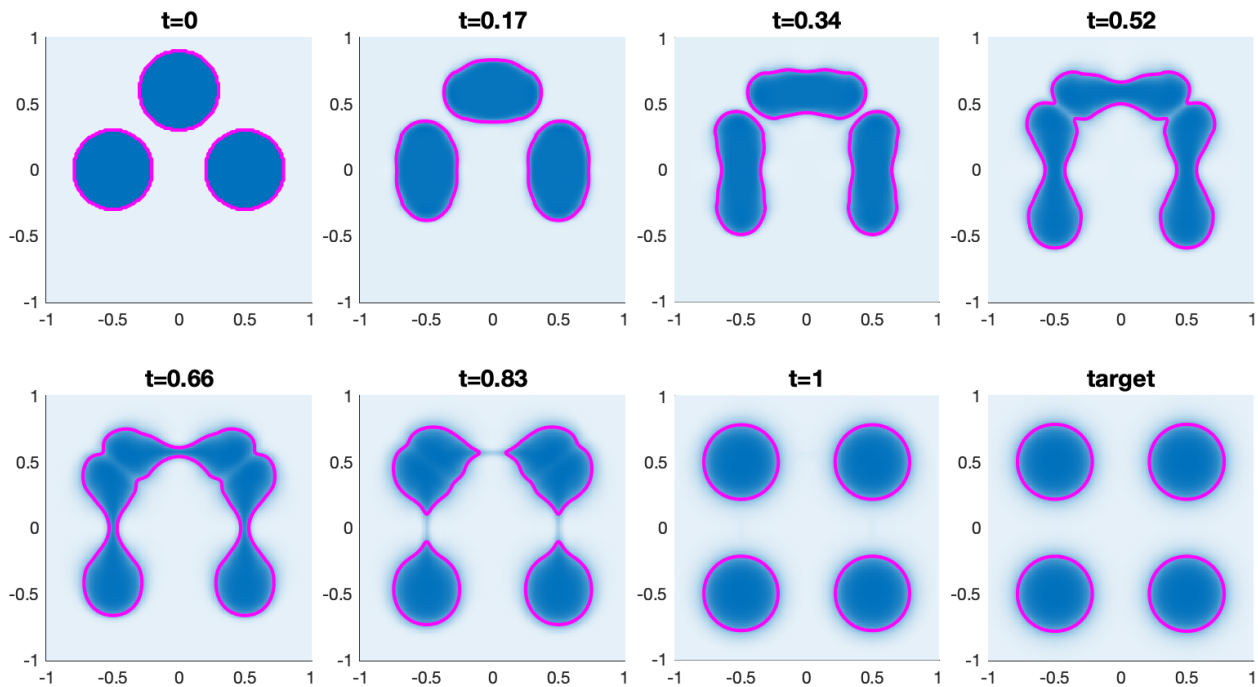


Figure 3: Here our initial shape was three unit disks and the final shape was four unit disks under a Gaussian blur. (Using default parameters.)

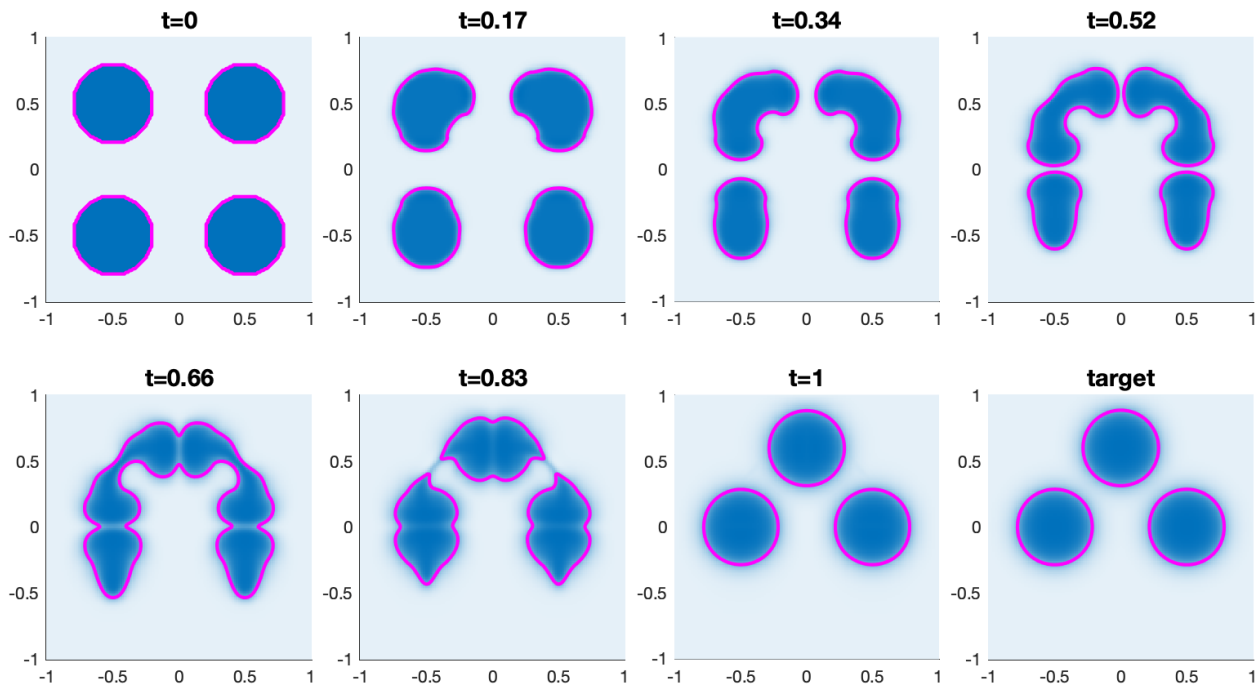


Figure 4: Reverse comparison from that of Figure 3. (Using default parameters.)

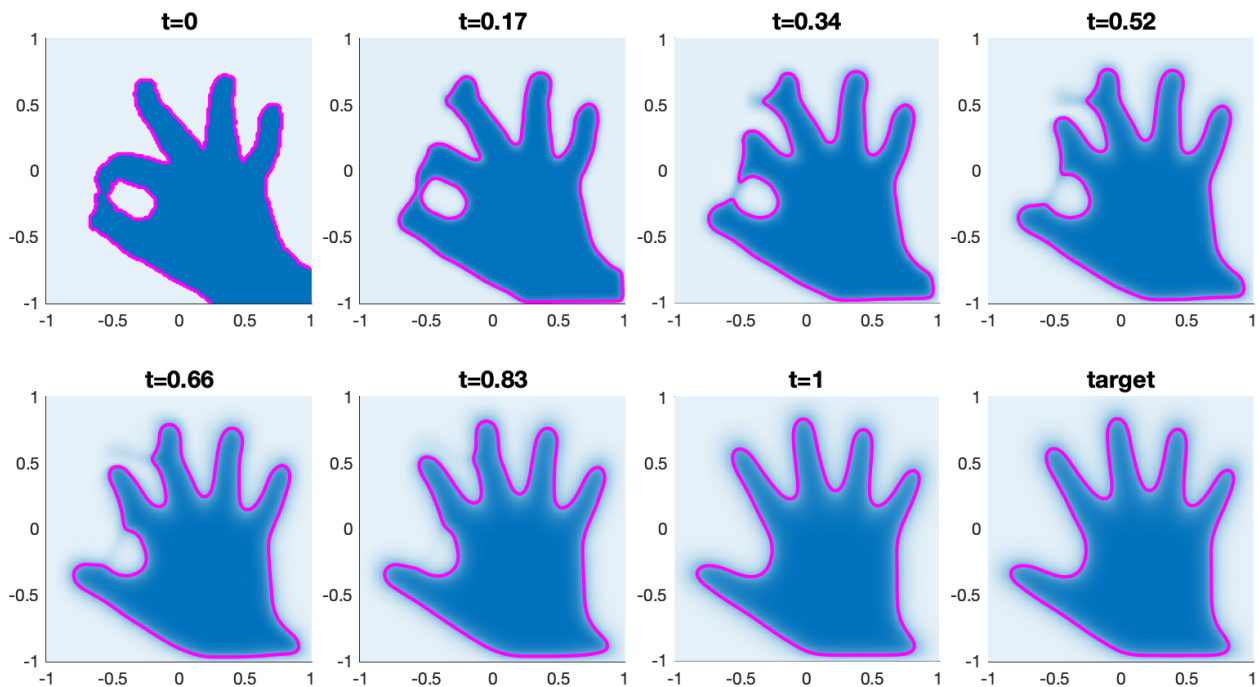


Figure 5: Here our initial shape was an hand giving the 'okay' gesture and the final shape was an open hand. (Using default parameters.)

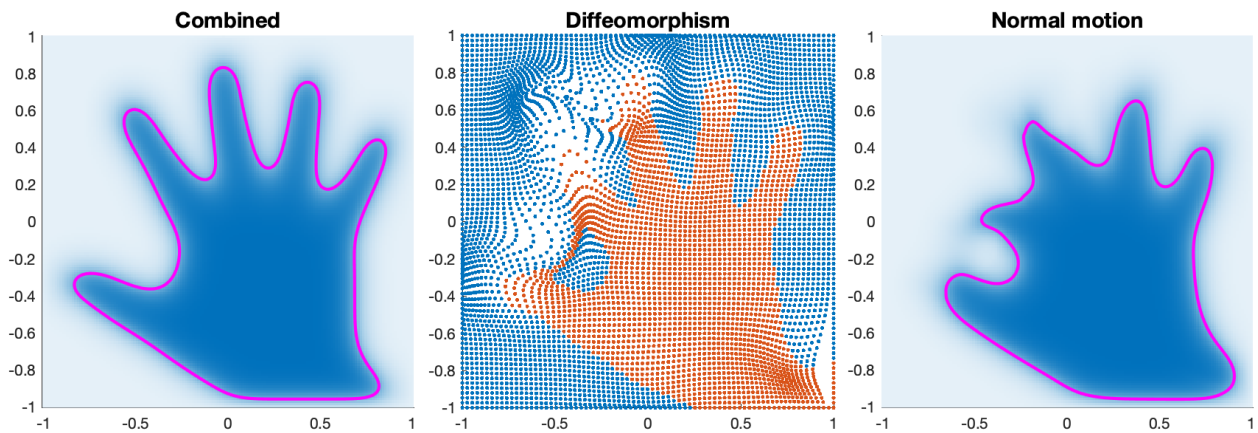


Figure 6: Visualization of the diffeomorphic and topological changes in the example of Figure 5.

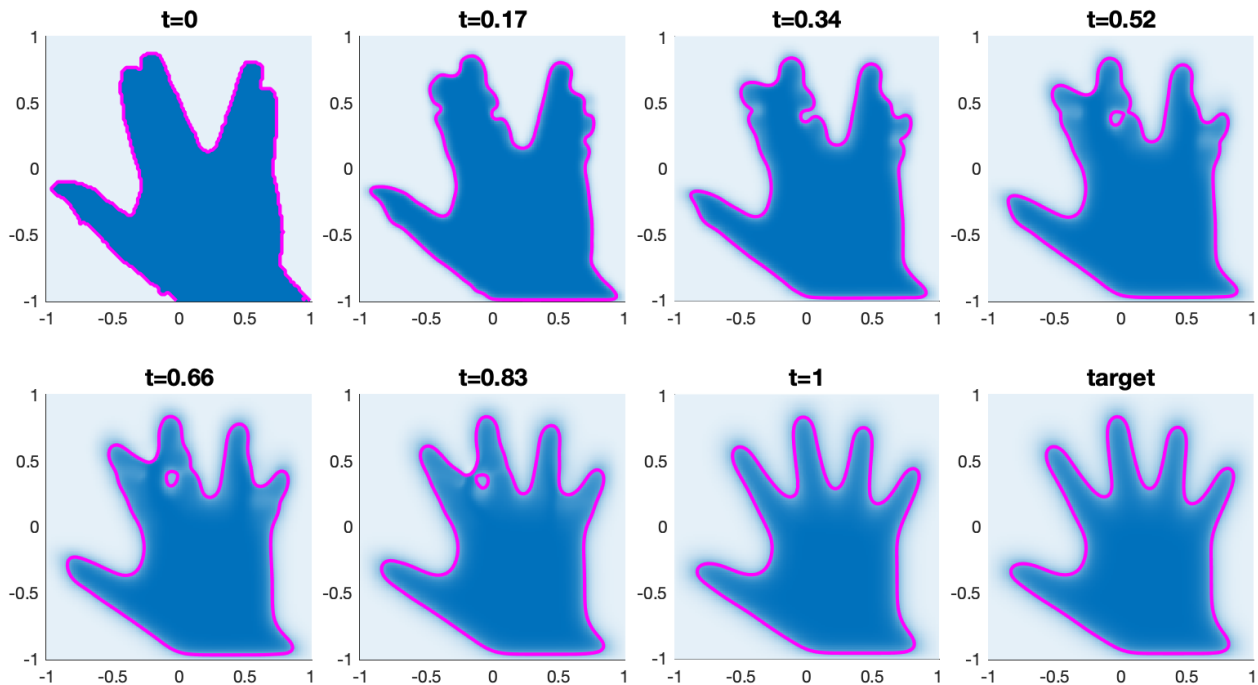


Figure 7: Here our initial shape is a hand with two pairs of fingers attached together and the last shape is an open hand, with $C_{\text{top}} = 10^6$ and default parameters otherwise.

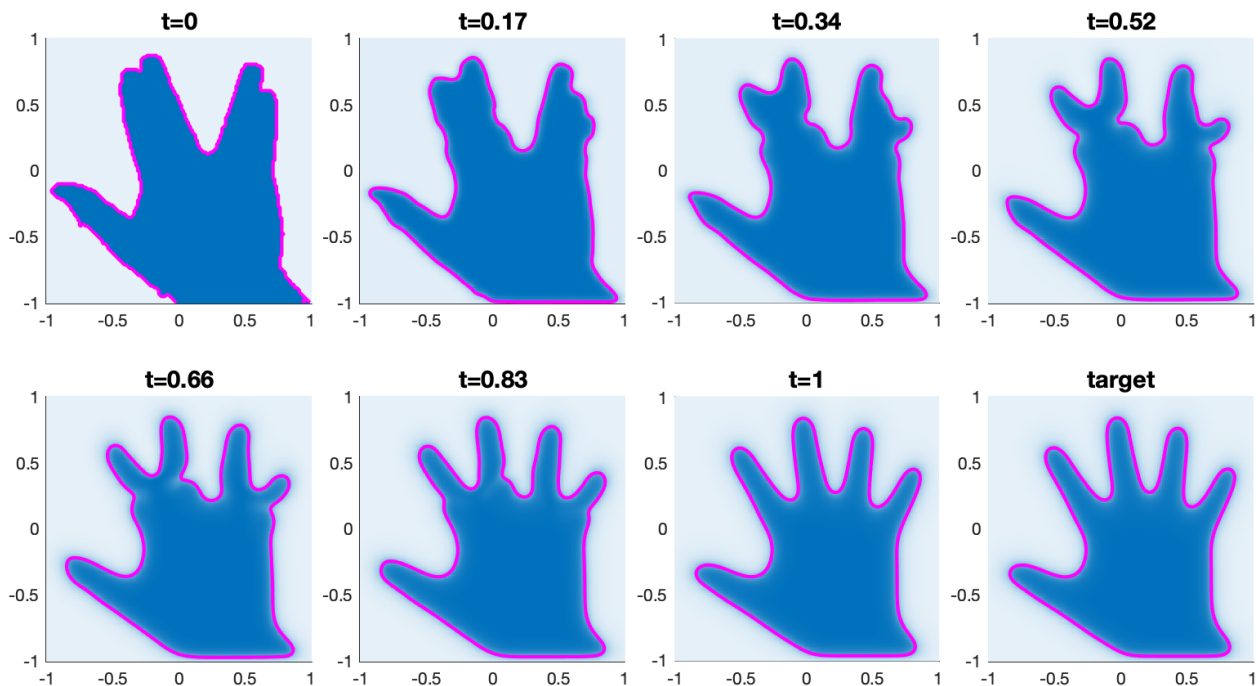


Figure 8: Same as Figure 7, with $C_{\text{top}} = 10^8$.

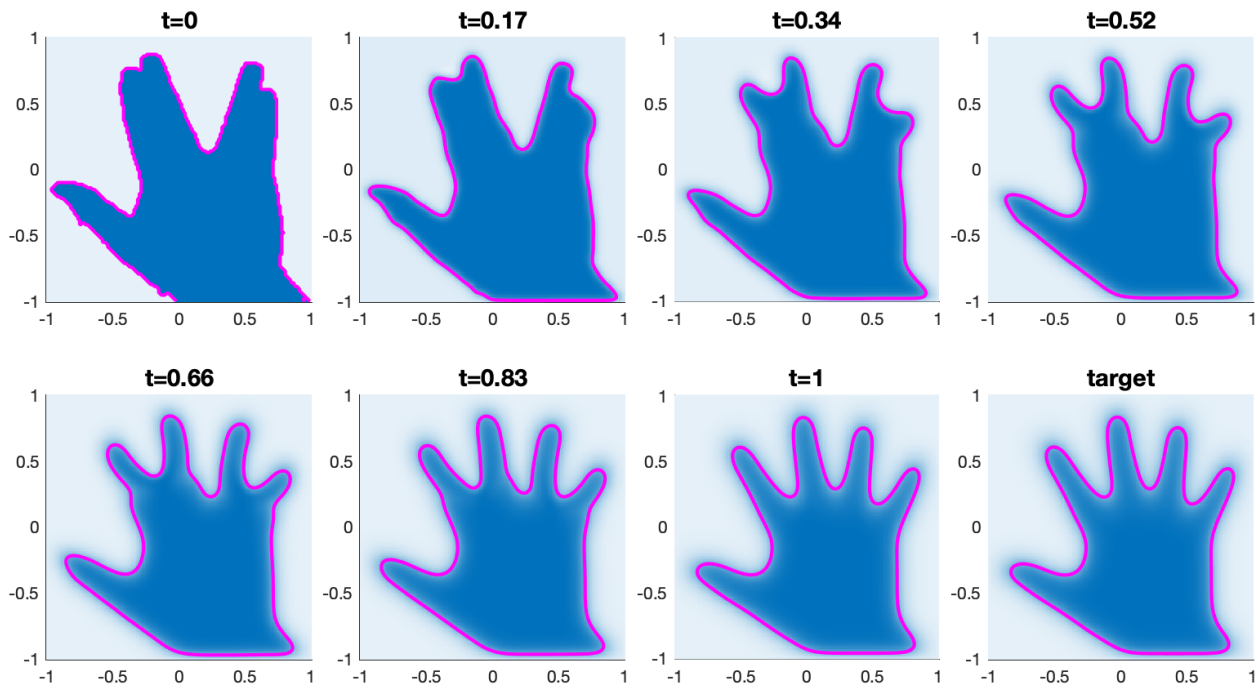


Figure 9: Same as Figure 7, with $C_{\text{top}} = 10^{10}$.

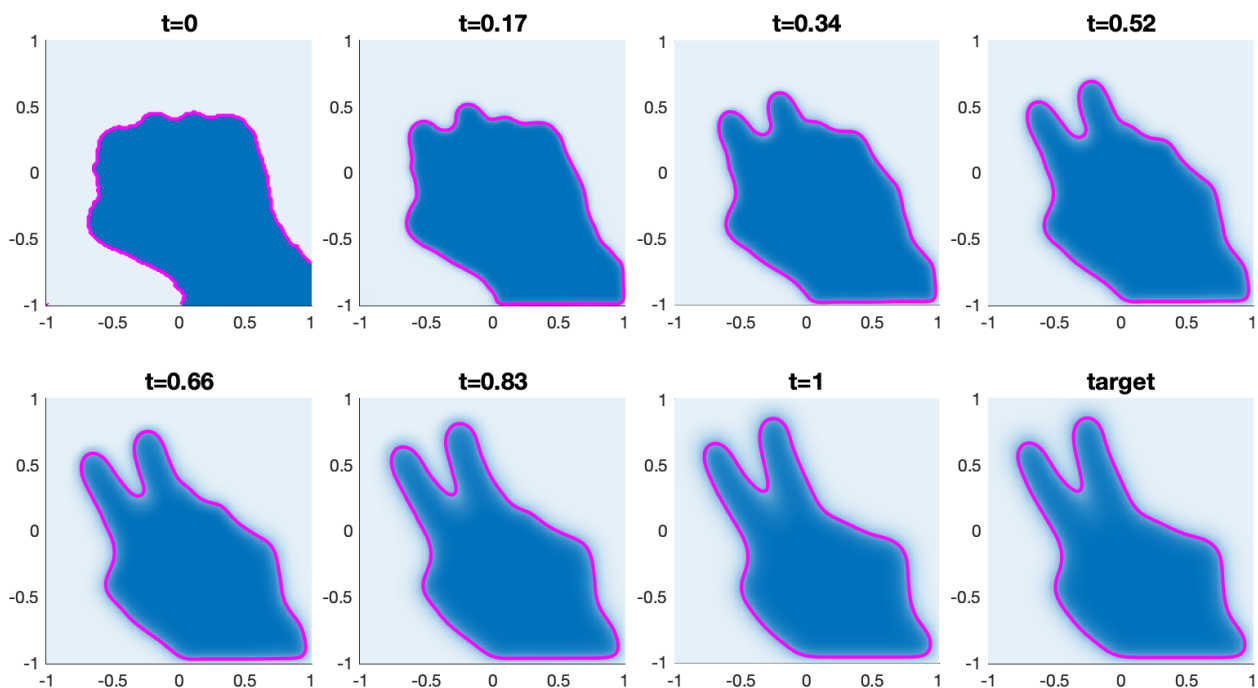


Figure 10: Here our initial shape is a hand with a closed fist and the target shape is a hand with two fingers up, the 'peace' gesture. (Using default parameters.)

of u and v . There are many open questions concerning this type of alignment. In particular what remains is proving the continuity of mild solutions with respect to the controls, the existence and uniqueness of strong solutions, and the existence of minimizers to the soft end point problem.

Acknowledgements

This research was partially funded at the Division of Applied Mathematics at Brown University by the NSF Research Training Grant: Mathematics of Information and Data with Applications to Science, the Brown Graduate School Presidential Fellowship, and Johns Hopkins University while D. Solano worked as an Assistant Research Engineer.

References

- [1] Helmut Abels. (non-) convergence of solutions of the convective allen–cahn equation. *Partial Differential Equations and Applications*, 3(1):1, 2022.
- [2] Ladyzhenskaya Olga Alexandrovna, Solonnikov Vsevolod Alekseevič, Ural’ceva Nina Nikolaevna, Smith S., and Olga Alexandrovna Ladyzhenskaya. *Linear and quasi-linear equations of parabolic type / by O. A. Ladyženskaja, V. A. Solonnikov, N. N. Ural’ceva ; [translated from Russian by S. Smith]*. Translations of mathematical monographs. American Mathematical Society, Providence, R.I, 1968.
- [3] Pierre-Louis Antonsanti, Joan Glaunès, Thomas Benseghir, Vincent Jugnon, and Irène Kaltenmark. Partial matching in the space of varifolds. In *International Conference on Information Processing in Medical Imaging*, pages 123–135. Springer, 2021.
- [4] V. I. Arnold. *Mathematical Methods of Classical Mechanics*. Springer, 1978. Second Edition: 1989.
- [5] John Ashburner. Computational anatomy with the spm software. *Magnetic resonance imaging*, 27(8): 1163–1174, 2009.
- [6] John Ashburner and Karl J Friston. Nonlinear spatial normalization using basis functions. *Human brain mapping*, 7(4):254–266, 1999.
- [7] Brian Avants, CL Epstein, and James C Gee. Geodesic image normalization in the space of diffeomorphisms. In *1st MICCAI Workshop on Mathematical Foundations of Computational Anatomy: Geometrical, Statistical and Registration Methods for Modeling Biological Shape Variability*, pages 125–135, 2006.
- [8] Martino Bardi and Italo Capuzzo-Dolcetta. *Optimal Control and Viscosity Solutions of Hamilton-Jacobi-Bellman Equations*. Modern Birkhäuser Classics. Birkhäuser Boston, MA, first edition, 1997. doi: <https://doi.org/10.1007/978-0-8176-4755-1>.
- [9] M. Bauer, M. Bruveris, and P.W. Michor. Overview of the geometries of shape spaces and diffeomorphism groups. *Journal of Mathematical Imaging and Vision*, 50:60–97, 2014. doi: <https://doi.org/10.1007/s10851-013-0490-z>.
- [10] Martin Bauer, Nicolas Charon, and Laurent Younes. Chapter 16 - metric registration of curves and surfaces using optimal control. In Ron Kimmel and Xue-Cheng Tai, editors, *Processing, Analyzing and Learning of Images, Shapes, and Forms: Part 2*, volume 20 of *Handbook of Numerical Analysis*, pages 613–646. Elsevier, 2019. doi: <https://doi.org/10.1016/bs.hna.2019.03.001>. URL <https://www.sciencedirect.com/science/article/pii/S1570865919300018>.

- [11] Mirza Faisal Beg, Michael Miller, Alain Trounev, and Laurent Younes. Computing large deformation metric mappings via geodesic flows of diffeomorphisms. *International Journal of Computer Vision*, 61: 139–157, 02 2005. doi: 10.1023/B:VISI.0000043755.93987.aa.
- [12] Haim Brezis and Haim Brézis. *Functional analysis, Sobolev spaces and partial differential equations*, volume 2. Springer, 2011.
- [13] Vicente Cervera, Francisca Mascaró, and Peter W. Michor. The action of the diffeomorphism group on the space of immersions. *Differential Geometry and its Applications*, 1(4):391–401, 1991. ISSN 0926-2245. doi: [https://doi.org/10.1016/0926-2245\(91\)90015-2](https://doi.org/10.1016/0926-2245(91)90015-2). URL <https://www.sciencedirect.com/science/article/pii/0926224591900152>.
- [14] Tony F Chan and Luminita A Vese. Active contours without edges. *IEEE TRANSACTIONS ON IMAGE PROCESSING*, 10(2), 2001.
- [15] Tony F Chan, Selim Esedoglu, and Mila Nikolova. Algorithms for finding global minimizers of image segmentation and denoising models. *SIAM journal on applied mathematics*, 66(5):1632–1648, 2006.
- [16] Gary E Christensen, Richard D Rabbitt, and Michael I Miller. Deformable templates using large deformation kinematics. *IEEE transactions on image processing*, 5(10):1435–1447, 1996.
- [17] M. Droske and M. Rumpf. A variational approach to non-rigid morphological registration. *SIAM Appl. Math.*, 64(2):668–687, 2004.
- [18] Qiang Du and Xiaobing Feng. Chapter 5 - the phase field method for geometric moving interfaces and their numerical approximations. In Andrea Bonito and Ricardo H. Nochetto, editors, *Geometric Partial Differential Equations - Part I*, volume 21 of *Handbook of Numerical Analysis*, pages 425–508. Elsevier, 2020. doi: <https://doi.org/10.1016/bs.hna.2019.05.001>. URL <https://www.sciencedirect.com/science/article/pii/S1570865919300043>.
- [19] Qiang Du, Lili Ju, Xiao Li, and Zhonghua Qiao. Maximum bound principles for a class of semilinear parabolic equations and exponential time-differencing schemes. *SIAM Review*, 63(2):317–359, 2021. doi: 10.1137/19M1243750. URL <https://doi.org/10.1137/19M1243750>.
- [20] P. Dupuis, U. Grenander, and M. Miller. Variational problems on flows of diffeomorphisms for image matching. *Quarterly of Appl. Math.*, 1998.
- [21] Lawrence C. Evans. *Partial Differential Equations*, volume 19.R of *Graduate Series in Mathematics*. American Mathematical Society, second edition, 2010.
- [22] Lawrence C Evans and Joel Spruck. Motion of level sets by mean curvature. i. In *Fundamental Contributions to the Continuum Theory of Evolving Phase Interfaces in Solids: A Collection of Reprints of 14 Seminal Papers*, pages 328–374. Springer, 1991.
- [23] W. H. Fleming and P. E. Souganidis. Asymptotic series and the method of vanishing viscosity. *Indiana University Mathematics Journal*, 35(2):425–447, 1986.
- [24] Karl Friston, John Ashburner, Christopher D Frith, J-B Poline, John D Heather, and Richard SJ Frackowiak. Spatial registration and normalization of images. *Human brain mapping*, 3(3):165–189, 1995.
- [25] M. Gage and R. S. Hamilton. The heat equation shrinking convex plane curves. *J. Differential Geometry*, 53:69–96, 1986.
- [26] Joan Glaunès, Anqi Qiu, Michael Miller, and Laurent Younes. Large deformation diffeomorphic metric curve mapping. *International journal of computer vision*, 80:317–336, 12 2008. doi: 10.1007/s11263-008-0141-9.

- [27] Malú Grave and Alvaro L.G.A. Coutinho. Comparing the convected level-set and the allen–cahn phase-field methods in amr/c simulations of two-phase flows. *Computers & Fluids*, 244:105569, 2022. ISSN 0045-7930. doi: <https://doi.org/10.1016/j.compfluid.2022.105569>. URL <https://www.sciencedirect.com/science/article/pii/S0045793022001888>.
- [28] M. Grayson. The heat equation shrinks embedded plane curves to round points. *J. Differential Geometry*, 26:285–314, 1987.
- [29] U. Grenander. *General Pattern Theory*. Oxford Science Publications, 1993.
- [30] U. Grenander and D. M. Keenan. On the shape of plane images. *Siam J. Appl. Math.*, 53(4):1072–1094, 1991.
- [31] U. Grenander and M. I. Miller. Computational anatomy: An emerging discipline. *Quarterly of Applied Mathematics*, LVI(4):617–694, 1998.
- [32] Daniel B. Henry. *Geometric Theory of Semilinear Parabolic Equations*, volume 840 of *Lecture Notes in Mathematics*. Springer, Berlin, 1981.
- [33] Darryl Holm, Alain Trounev, and Laurent Younes. The euler-poincaré theory of metamorphosis. *Quarterly of Applied Mathematics*, 67(4):661–685, 2009.
- [34] Hsi-Wei Hsieh and Nicolas Charon. Weight metamorphosis of varifolds and the lddmm-fisher-rao metric. *Calculus of Variations and Partial Differential Equations*, 61(5):165, 2022.
- [35] Guang-Shan Jiang and Chi-Wang Shu. Efficient implementation of weighted eno schemes. *Journal of Computational Physics*, 126(1):202–228, 1996. ISSN 0021-9991. doi: <https://doi.org/10.1006/jcph.1996.0130>. URL <https://www.sciencedirect.com/science/article/pii/S0021999196901308>.
- [36] Sarang Joshi and Michael Miller. Landmark matching via large deformation diffeomorphisms. *IEEE transactions on image processing : a publication of the IEEE Signal Processing Society*, 9:1357–70, 02 2000. doi: 10.1109/83.855431.
- [37] Maximilian Kloppe and Sebastian Aland. A phase-field model of elastic and viscoelastic surfaces in fluids. *Computer Methods in Applied Mechanics and Engineering*, 428:117090, 2024. ISSN 0045-7825. doi: <https://doi.org/10.1016/j.cma.2024.117090>. URL <https://www.sciencedirect.com/science/article/pii/S0045782524003463>.
- [38] Gary M. Lieberman. The first initial-boundary value problem for quasilinear second order parabolic equations. *Annali della Scuola Normale Superiore di Pisa - Classe di Scienze*, Ser. 4, 13(3):347–387, 1986. URL http://www.numdam.org/item/ASNSP_1986_4_13_3_347_0/.
- [39] Ravi Malladi, James A Sethian, and Baba C Vemuri. Shape modeling with front propagation: A level set approach. *IEEE transactions on pattern analysis and machine intelligence*, 17(2):158–175, 2002.
- [40] Peter W Michor. Some geometric evolution equations arising as geodesic equations on groups of diffeomorphisms including the hamiltonian approach. *Phase space analysis of partial differential equations*, pages 133–215, 2007.
- [41] MI Miller and L Younes. Group actions, homeomorphisms, and matching: A general framework. *International Journal of Computer Vision*, 41(1-2):61–84, 2001.
- [42] Diana Nunziante. Existence and uniqueness of unbounded viscosity solutions of parabolic equations with discontinuous time-dependence. *Nonlinear Analysis: Theory, Methods & Applications*, 18(11):1033–1062, 1992. ISSN 0362-546X. doi: [https://doi.org/10.1016/0362-546X\(92\)90194-J](https://doi.org/10.1016/0362-546X(92)90194-J). URL <https://www.sciencedirect.com/science/article/pii/0362546X9290194J>.

- [43] Stanley Osher and Ronald P Fedkiw. Level set methods: an overview and some recent results. *Journal of Computational physics*, 169(2):463–502, 2001.
- [44] Stanley Osher and James A Sethian. Fronts propagating with curvature-dependent speed: Algorithms based on hamilton-jacobi formulations. *Journal of Computational Physics*, 79(1):12–49, 1988. ISSN 0021-9991. doi: [https://doi.org/10.1016/0021-9991\(88\)90002-2](https://doi.org/10.1016/0021-9991(88)90002-2). URL <https://www.sciencedirect.com/science/article/pii/0021999188900022>.
- [45] Stanley Osher, Ronald Fedkiw, and Krzysztof Piechor. Level set methods and dynamic implicit surfaces. *Appl. Mech. Rev.*, 57(3):B15–B15, 2004.
- [46] Casey Richardson and Laurent Younes. Metamorphosis of images in reproducing kernel hilbert spaces. *Advances in Computational Mathematics*, 42, 06 2016. doi: 10.1007/s10444-015-9435-y.
- [47] Casey L Richardson and Laurent Younes. Computing metamorphoses between discrete measures. *Journal of Geometric Mechanics*, 5(1):131–150, 2013.
- [48] James A Sethian. Theory, algorithms, and applications of level set methods for propagating interfaces. *Acta numerica*, 5:309–395, 1996.
- [49] Jie Shen, Tao Tang, and Jiang Yang. On the maximum principle preserving schemes for the generalized allen–cahn equation. *Communications in Mathematical Sciences*, 14:1517–1534, 01 2016. doi: 10.4310/CMS.2016.v14.n6.a3.
- [50] Chi-Wang Shu and Stanley Osher. Efficient implementation of essentially non-oscillatory shock-capturing schemes. *Journal of Computational Physics*, 77(2):439–471, 1988. ISSN 0021-9991. doi: [https://doi.org/10.1016/0021-9991\(88\)90177-5](https://doi.org/10.1016/0021-9991(88)90177-5). URL <https://www.sciencedirect.com/science/article/pii/0021999188901775>.
- [51] Yashil Sukurdeep, Martin Bauer, and Nicolas Charon. A new variational model for shape graph registration with partial matching constraints. *SIAM Journal on Imaging Sciences*, 15(1):261–292, 2022.
- [52] Michael E. Taylor. *Partial Differential Equations III*. Applied Mathematical Sciences. Springer New York, NY, 2011. doi: <https://doi.org/10.1007/978-1-4419-7049-7>.
- [53] D’Arcy Wendworth Thompson. *On Growth and Form*. Dover Publications, 1917. Revised edition 1992.
- [54] A. Trouvé. Habilitation à diriger les recherches. Technical report, Université Paris XI, 1996.
- [55] A. Trouvé. Diffeomorphism groups and pattern matching in image analysis. *Int. J. of Comp. Vis.*, 28(3):213–221, 1998.
- [56] Alain Trouvé and Laurent Younes. Local geometry of deformable templates. *SIAM journal on mathematical analysis*, 37(1):17–59, 2005.
- [57] Alain Trouvé and Laurent Younes. Metamorphoses through lie group action. *Foundations of computational mathematics*, 5:173–198, 2005.
- [58] Marc Vaillant and Joan Glaunès. Surface matching via currents. volume 19, pages 381–92, 02 2005. ISBN 978-3-540-26545-0. doi: 10.1007/11505730_32.
- [59] Tom Vercauteren, Xavier Pennec, Aymeric Perchant, and Nicholas Ayache. Diffeomorphic demons: Efficient non-parametric image registration. *NeuroImage*, 45(1):S61–S72, 2009.
- [60] Luminita A Vese and Tony F Chan. A multiphase level set framework for image segmentation using the mumford and shah model. *International journal of computer vision*, 50:271–293, 2002.

- [61] Fred B Weissler. Semilinear evolution equations in banach spaces. *Journal of Functional Analysis*, 32(3):277–296, 1979. ISSN 0022-1236. doi: [https://doi.org/10.1016/0022-1236\(79\)90040-5](https://doi.org/10.1016/0022-1236(79)90040-5). URL <https://www.sciencedirect.com/science/article/pii/0022123679900405>.
- [62] Fred B. Weissler. Local existence and nonexistence for semilinear parabolic equations in l_p . *Indiana University Mathematics Journal*, 29(1):79–102, 1980. ISSN 00222518, 19435258. URL <http://www.jstor.org/stable/24892566>.
- [63] Fred B. Weissler. Existence and non-existence of global solutions for a semilinear heat equation. *Israel Journal of Mathematics*, 38:29–40, 1981. URL <https://api.semanticscholar.org/CorpusID:122167438>.
- [64] Li Xunjing and Jiongmin Yong. *Optimal Control Theory for Infinite Dimensional Systems*. Systems & Control: Foundations & Applications. Birkhäuser Boston, MA, first edition, 1995. doi: <https://doi.org/10.1007/978-1-4612-4260-4>.
- [65] Laurent Younes. Computable elastic distances between shapes. *SIAM Journal on Applied Mathematics*, 58(2):565–586, 1998. ISSN 00361399. URL <http://www.jstor.org/stable/118345>.
- [66] Laurent Younes. *Shapes and Diffeomorphisms*. Number 171 in Applied Mathematical Sciences. Springer, second edition, 2019.